Infrared spatial interferometer (ISI) scientists, technicians, students

C.H. Townes W. Fitelson

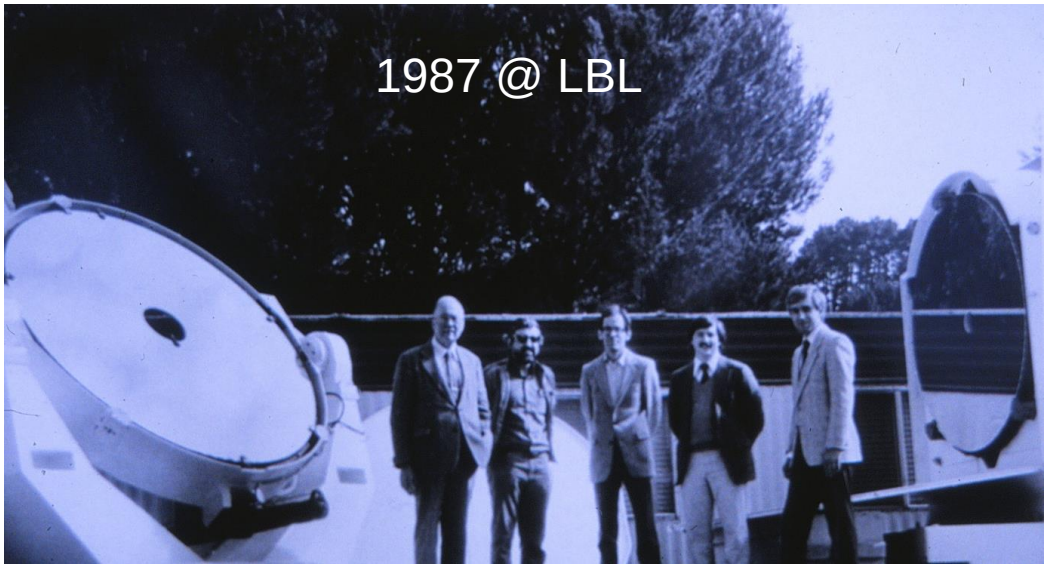

K.S. Abdeli
M. Bester
A.A. Chandler
J. Cobb
W.C. Danchi
C.G. Degiacomi
R. Fulton
L.J. Greenhill
R.L. Griffith
D.D.S. Hale*
S. Hoss
M. Johnson*
E.A. Lipman*
S. Lockwood
B. Lopez
T. MacDonald
J. McMahon
J.D. Monnier*
B. Saduolet
J. Storey
K. Tatebe*
S. Tevousian*
P.G. Tuthill
K. Reichl
J. Remy
C.S. Ryan
J. Shapiro
E.C. Sutton*
V. Toy
J. Weiner*
R.H. Weitzman
E.H. Wishnow
and many more…

Grad students get a *

ISI principle of operation: Definition of “Visibility”

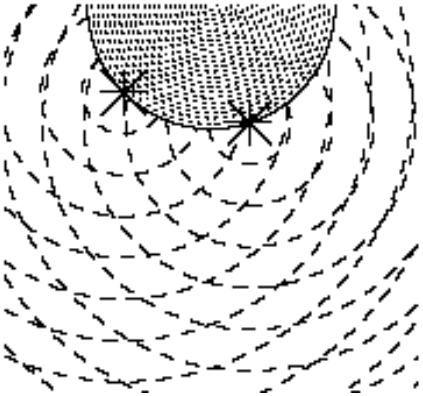

$$V_{ij} = \frac{I_{max} - I_{min}}{I_{max} + I_{min}},$$

$$V_{ij}^2 = \frac{|F_{ij}|^2}{P_i P_j}.$$

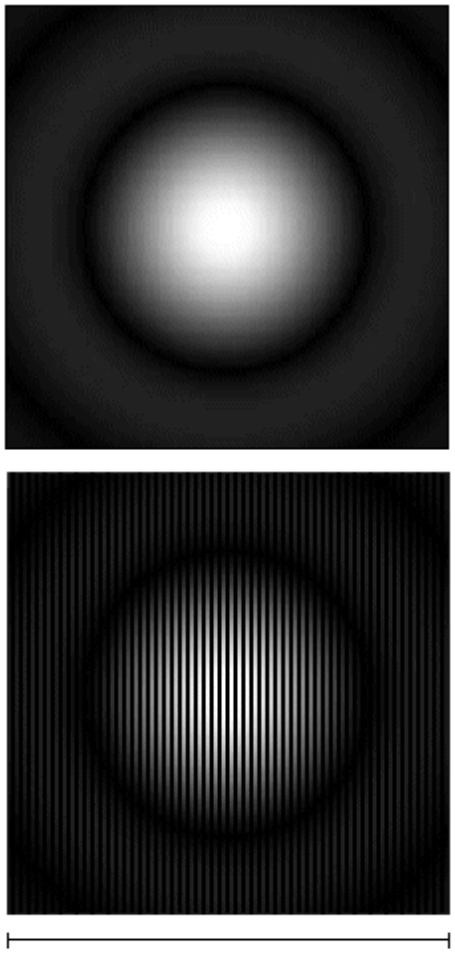

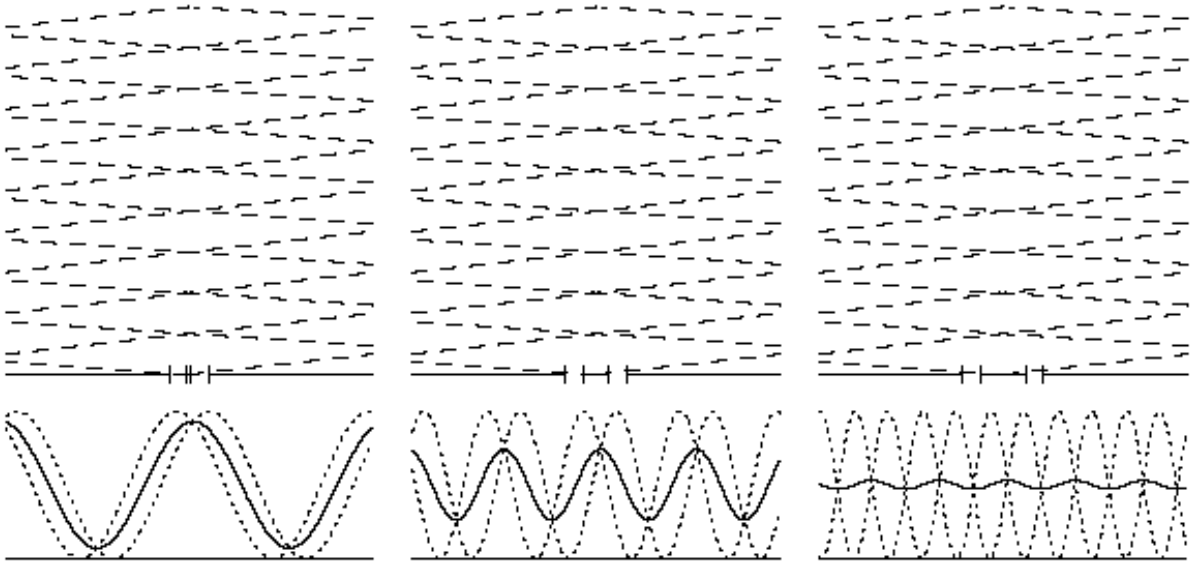

Van Cittert-Zernike theorem:
Visibility = $\mathcal{FT}$ brightness dist.
Visibility is the spatial autocorrelation function

Weiner, 2002

Michelson Stellar Interferometer Mt. Wilson 100”

Michelson and Pease, 1921

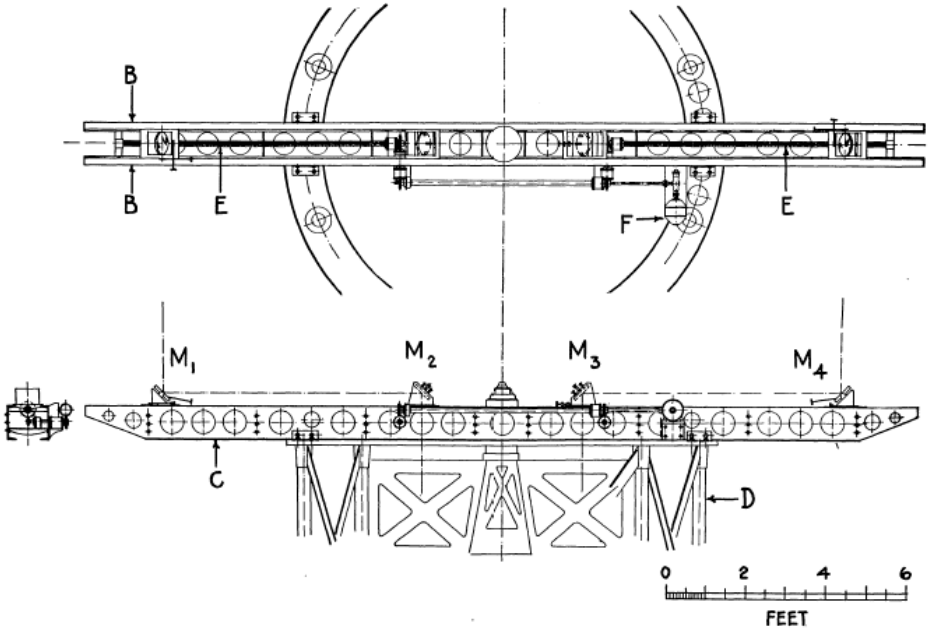

FIG. 2.—Diagram of 20-foot interferometer beam. M_1, M_2, M_3, M_4, mirrors; B, B, 10-inch channels; C, steel plate; E, E, screws to move outer mirrors; F, motor drive for screws; D, Cassegrain cage.

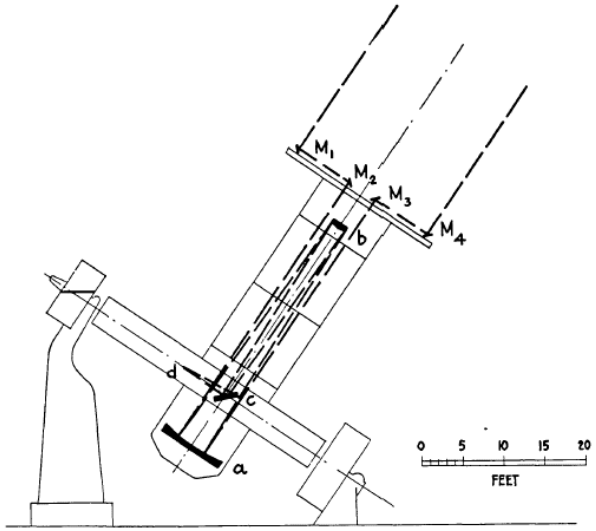

FIG. 1.—Diagram of optical path of interferometer pencils. M_1, M_2, M_3, M_4, mirrors; a, 100-inch paraboloid; b, convex mirror; c, coudé flat; d, focus.

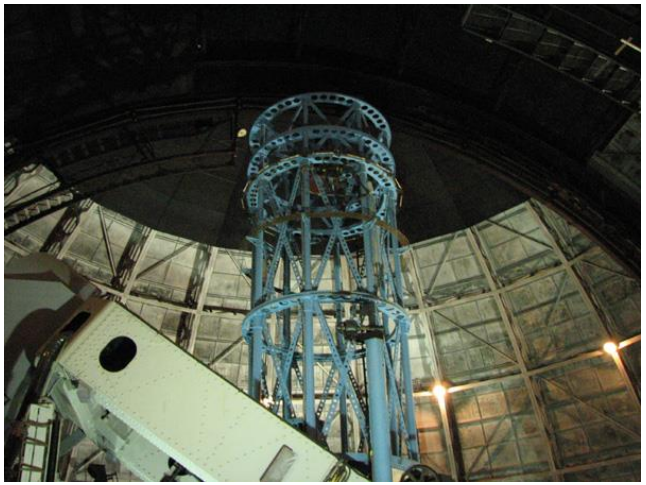

Demonstration at McMath-Pierce tele. Kitt Peak

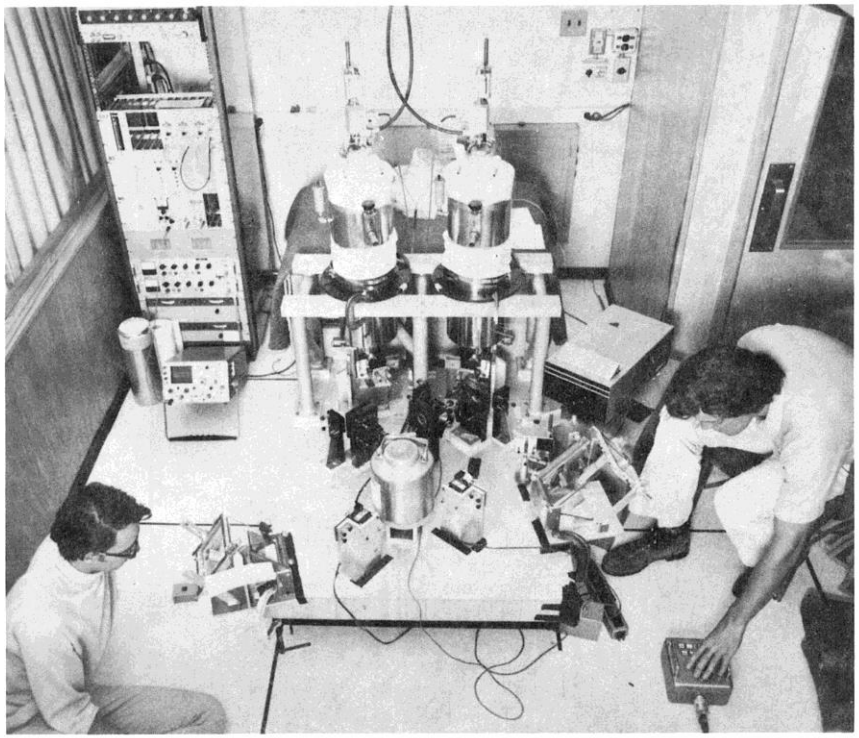

Mid-IR (10 μm) interferometry using heterodyne detection.
5.5 m baseline separation between auxiliary siderostats
Mike Johnson, Al Betz, Charles Townes
Phys. Rev. Lett, 33, 1617, 1974
Atmosphere shown to be stable enough for coherence and interference fringes from Mercury detected.

ISI characteristics

Pfund optical design

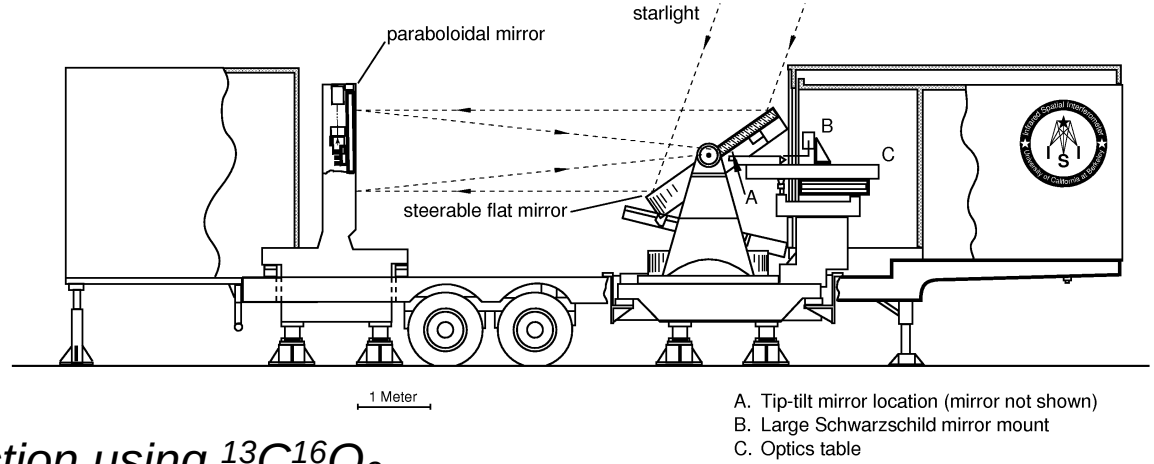

Heterodyne detection using $^{13}C^{16}O_2$ lasers as local oscillators

Geometric delays removed using RF delay lines

Mid-IR penetrates dust to observe star & also observes optically thin dust shell
Narrow spectral bandwidth +/- 2.6 GHz

In operation at Mt. Wilson 1988
First fringes 1989
Third telescope 2003
Closure phase measured 2004

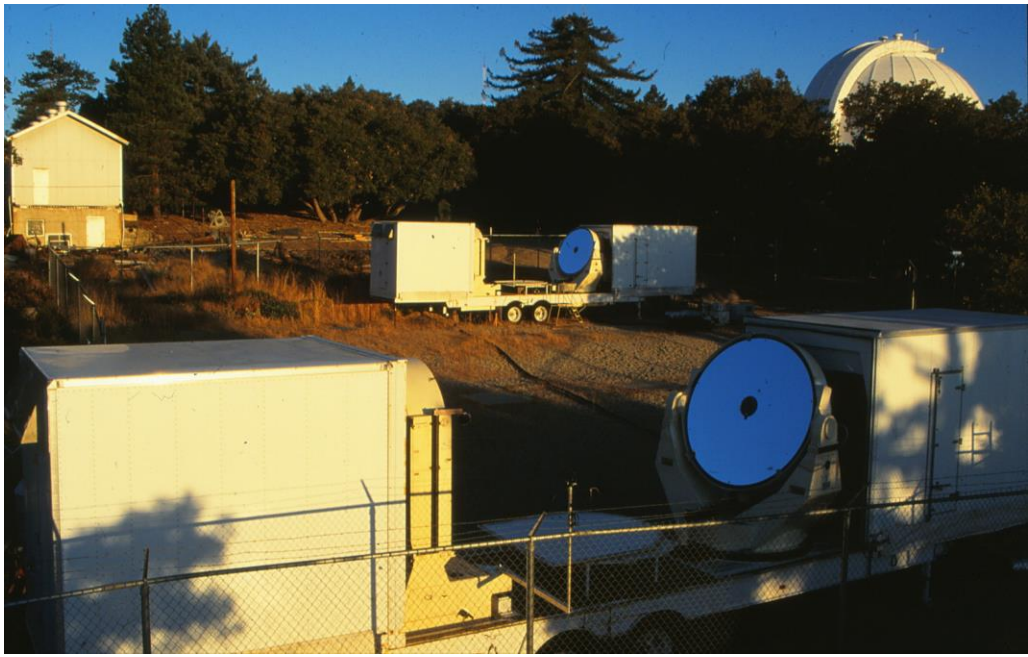

2 telescope system ~30m baseline 1994

Interferometer schematic, examples of fringes

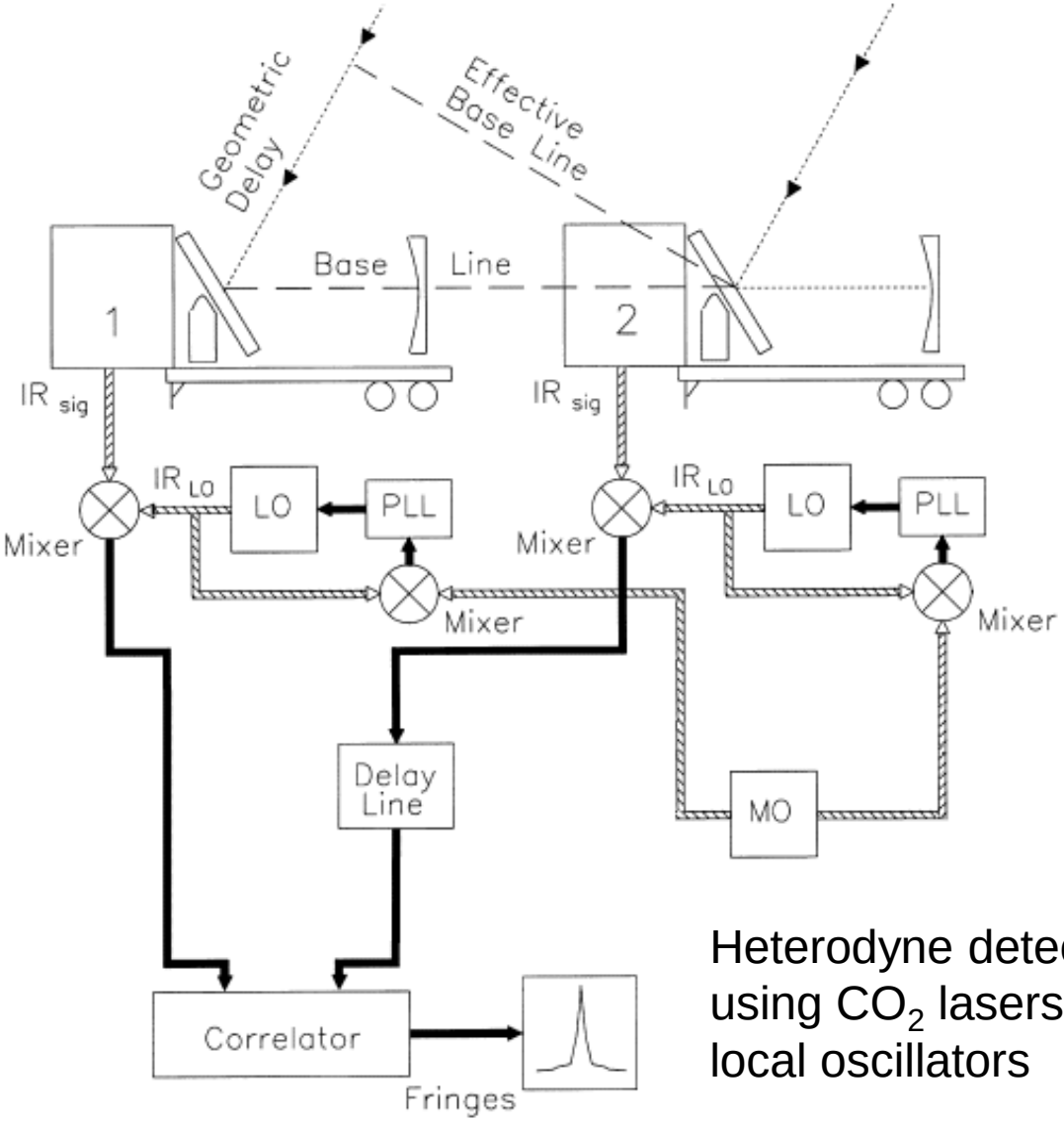

Heterodyne detection using CO_2 lasers as local oscillators

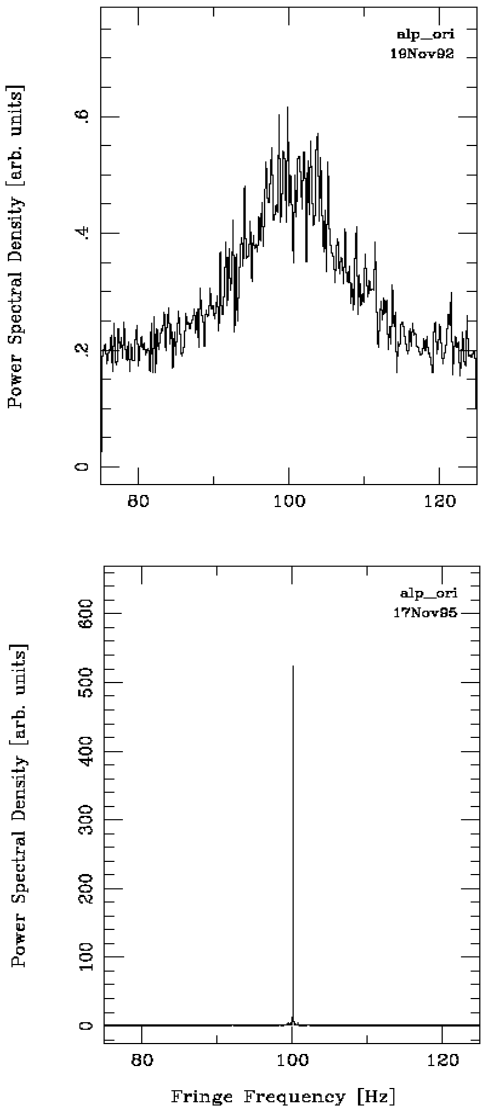

Example of measured visibility function

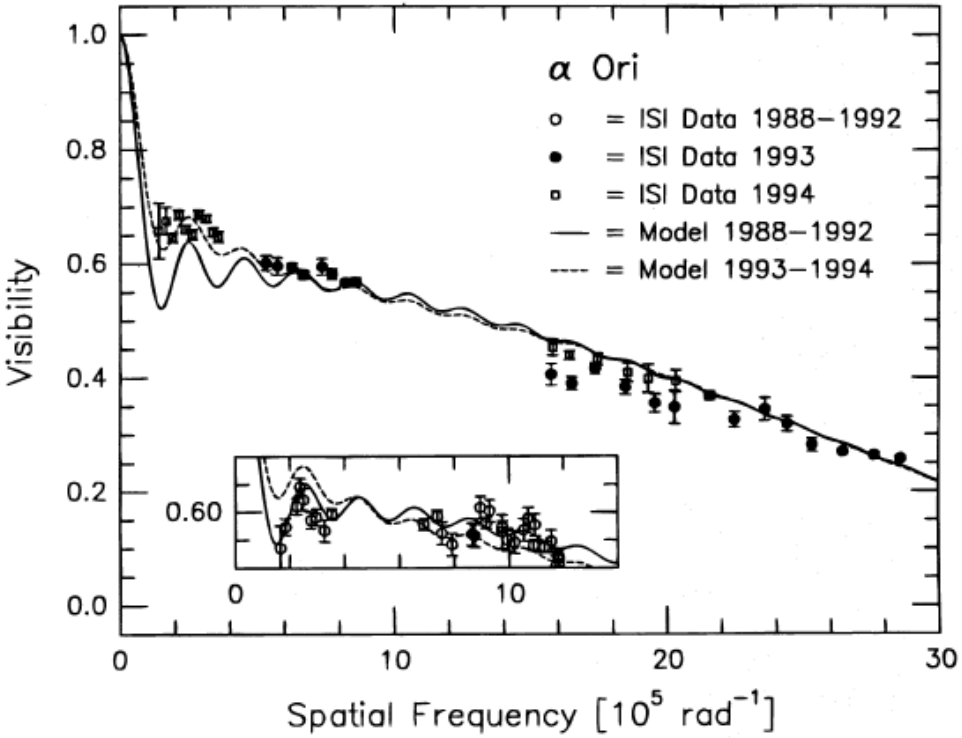

Fringe visibility measured over various baseline distances.

Spatial frequency in units of 10^5 cycles/radian

Two main components to the visibility curve: stellar and dust.

ISI site and moving telescopes

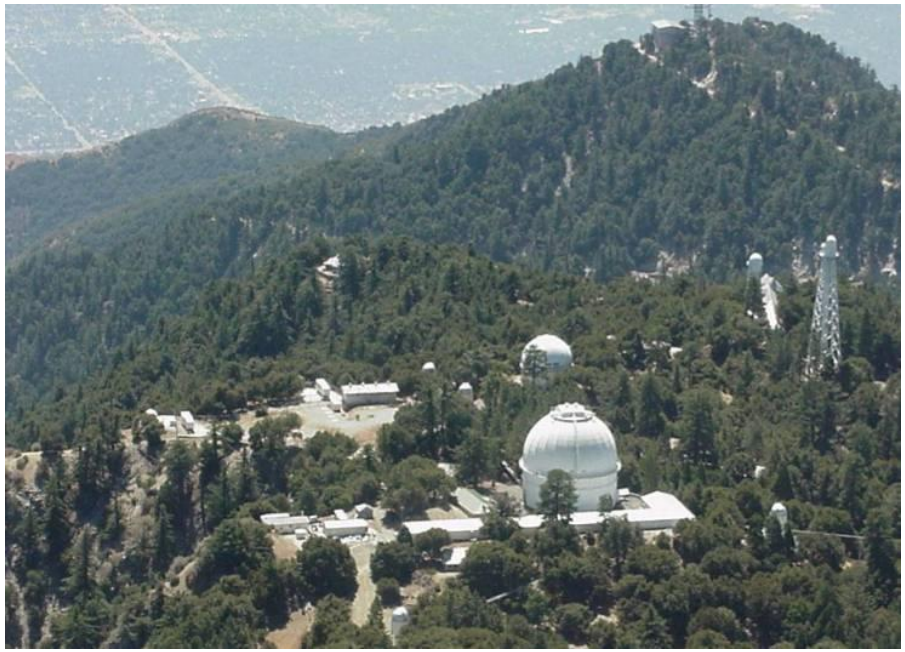

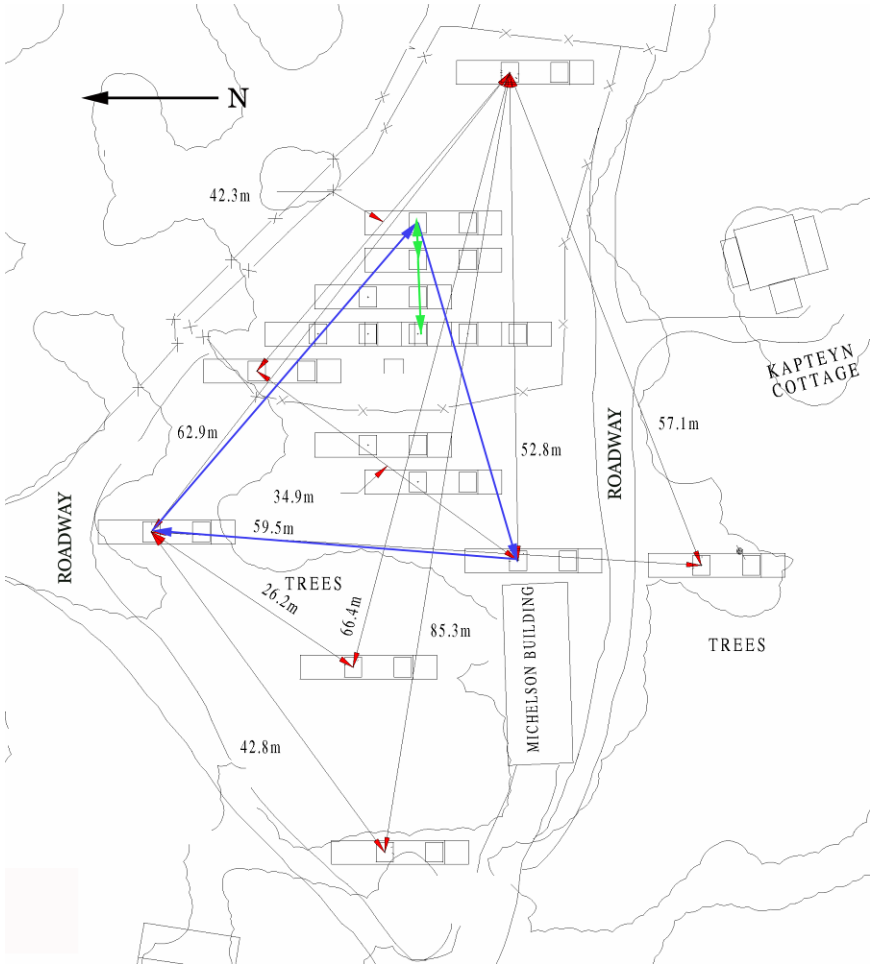

Baselines from 4 to 85 m

ISI three telescope array

3 telescope system 4,8,12m EW baselines 2005
Currently ~35m triangular baselines

Current system, spectrometer taps A1,A2,A3

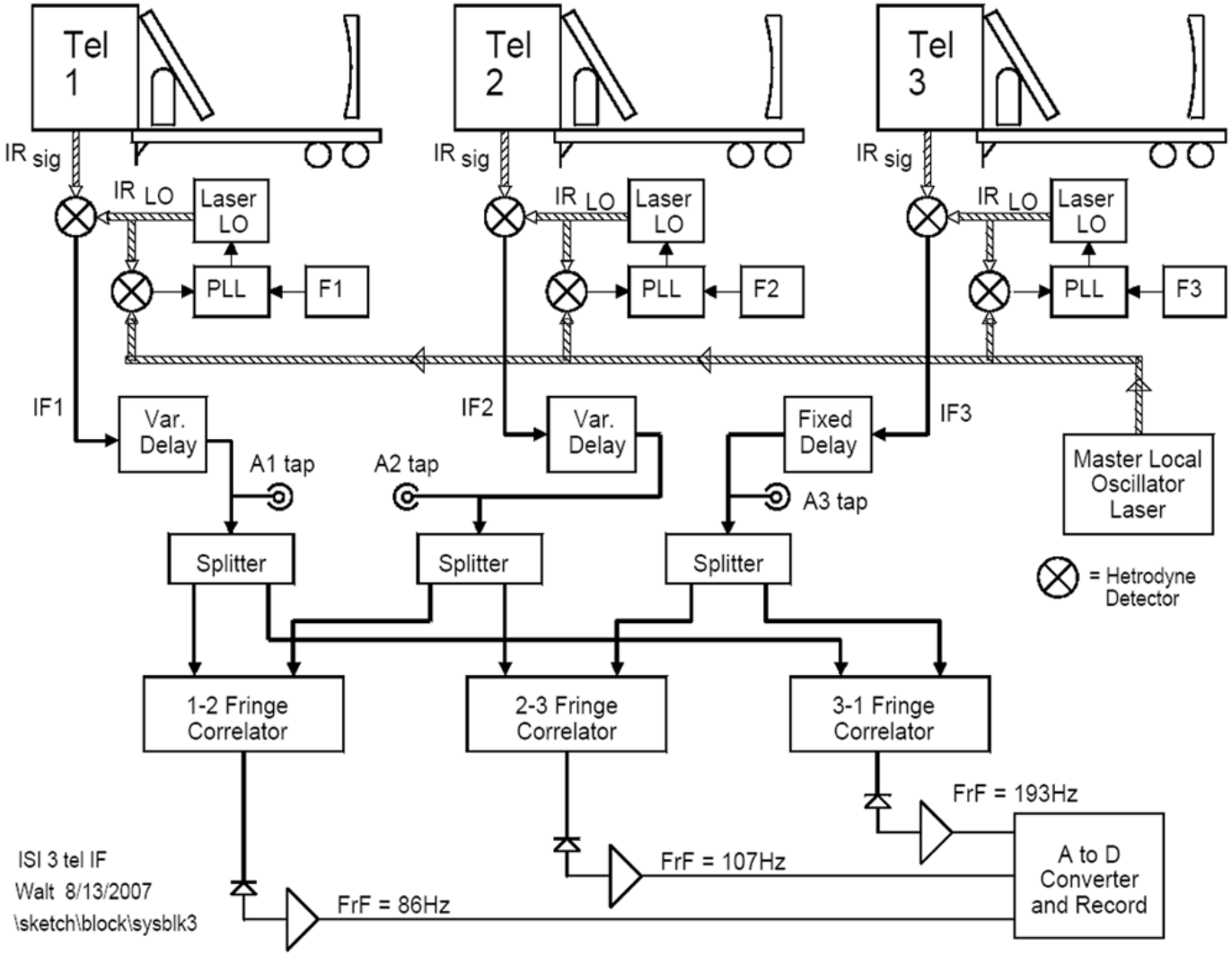

Red Giant and Asymptotic Giant Branch stars

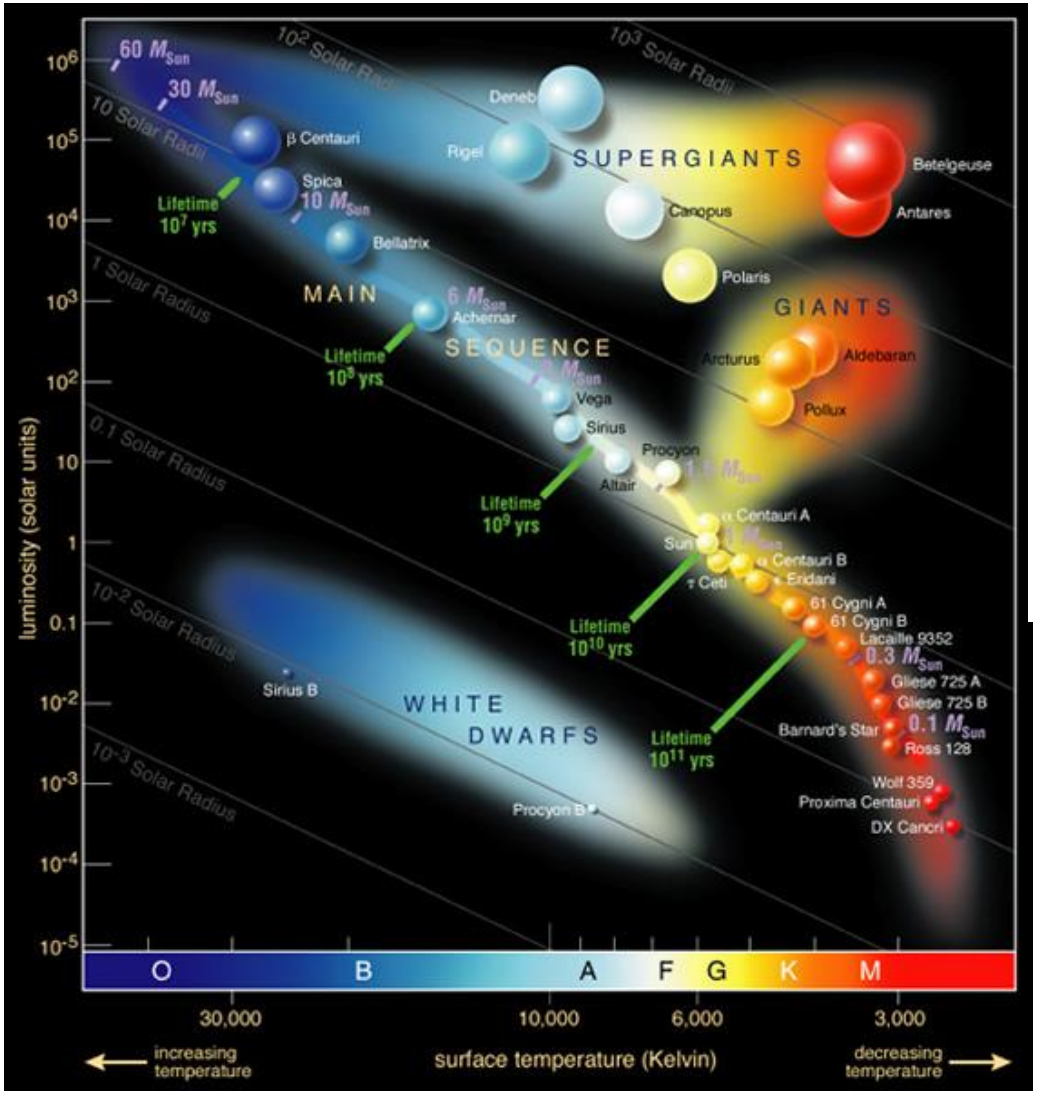

Bramboroson.com

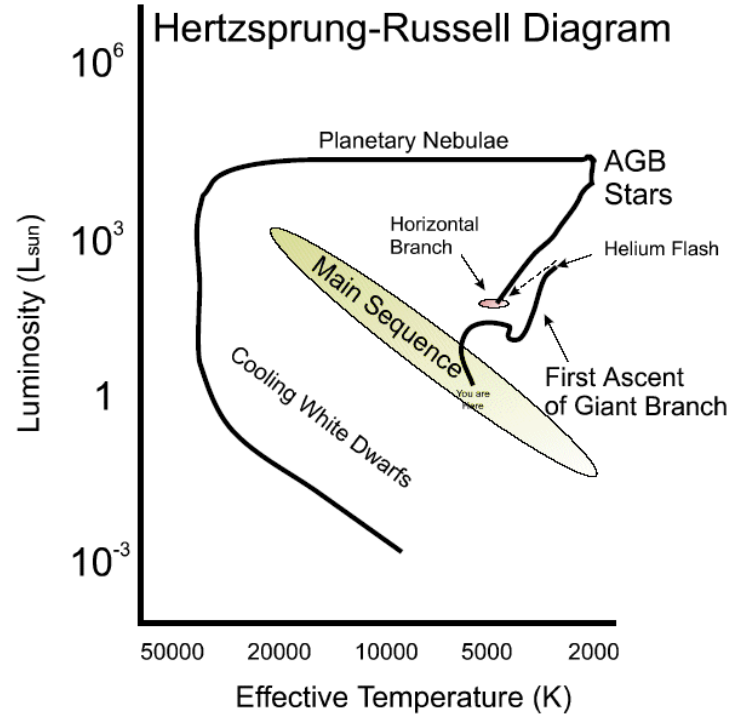

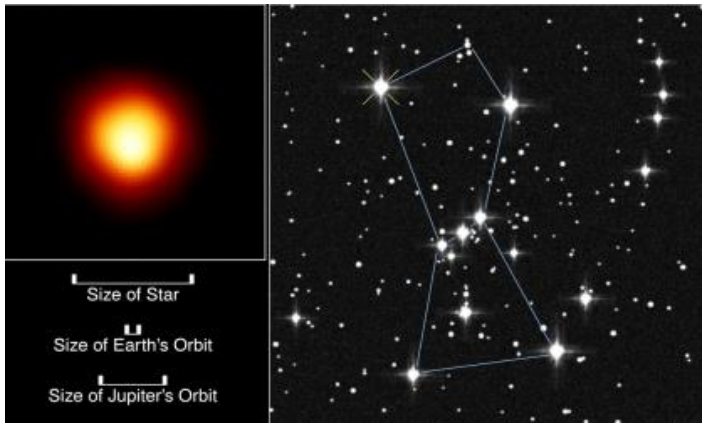

Atmosphere of Betelgeuse - Alpha Orionis
Hubble Space Telescope - Faint Object Camera
January 15, 1996; A. Dupree (CfA), NASA, ESA

Intensity variations of Mira variables

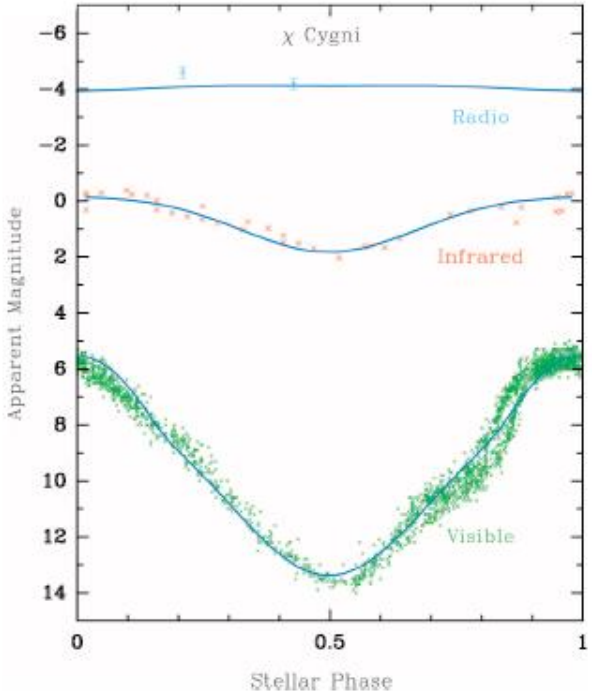

Mira (o ceti), M7 III spectral class
Ang. size: ~0.”045 diameter (11.15 um)
@ distance of 110 parsec= 5.0 A.U.
Mass: ~1 Msolar
Temperature: ~3000 K
Period ~330 days
Surface grav. log(g)~0.5
~10000 less than solar

Surrounded by gas and dust
Source of C,N,O to ISM

Discovered by Fabricius 1596
Mira means “Wonderful” in Latin

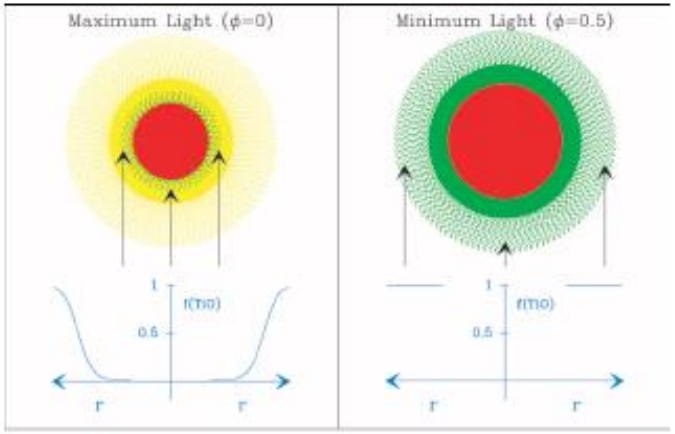

Vis. & NIR (1 um) changes due to forming and dissociation of TiO (& others)

Reid & Goldston 2002 ApJ, 568, 931

Galex UV 151.6 nm
Martin 2007 Nature

Aspects of Red Giant & Mira stars: Opacity

Measured size varies with wavelength

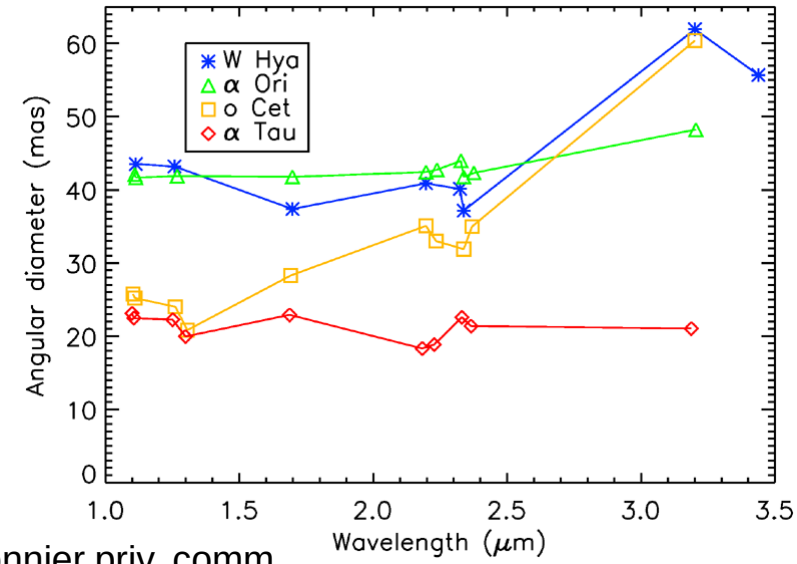

Monnier priv. comm.

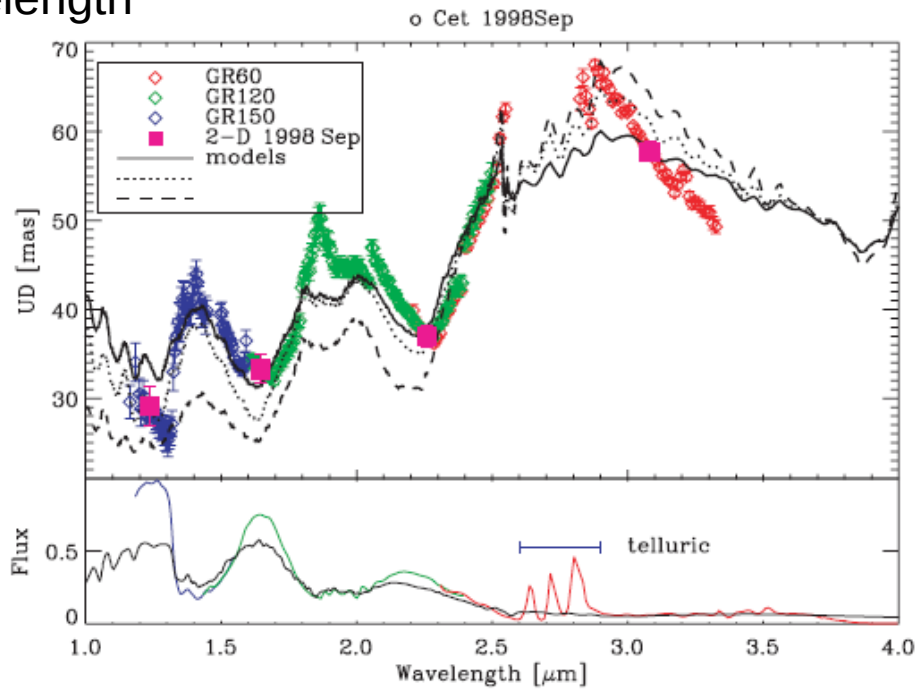

Size and shape varies in time, simulation of Mira

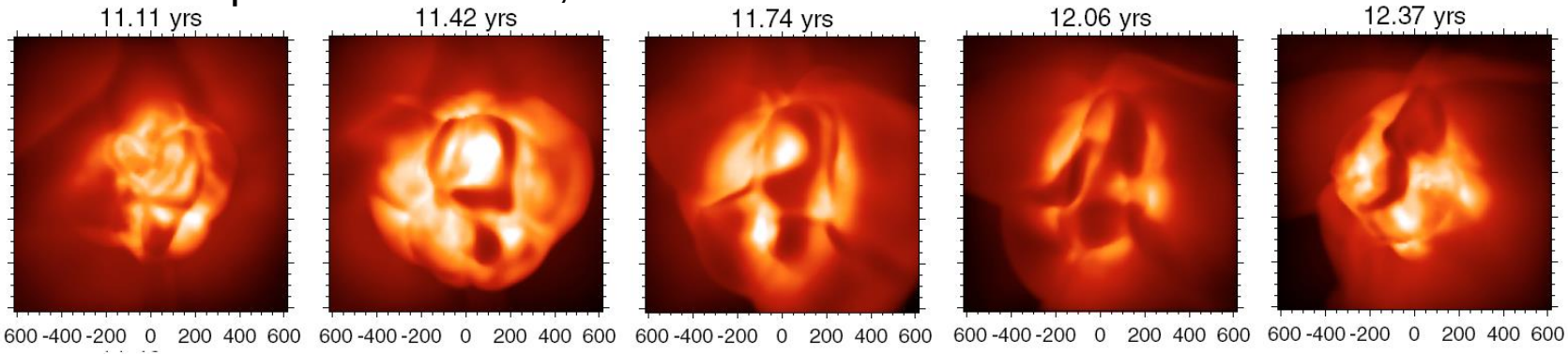

Freytag & Hofner, A&A, 483, 571 2008

Variations in dust shells and stellar sizes

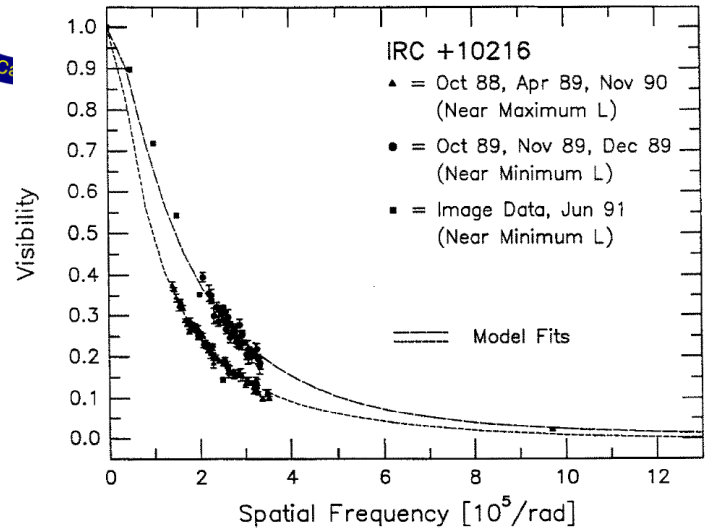

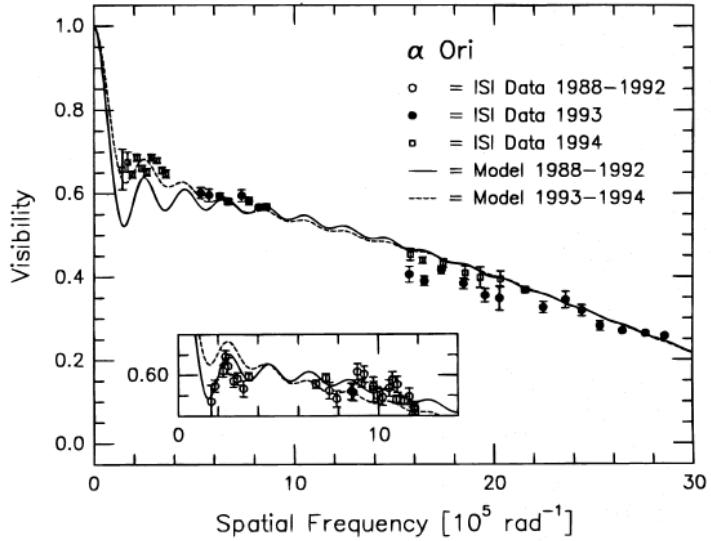

IRC+10216, Variation of visibilities
Betelgeuse, Visibility dust and stellar parts
Bester et al. 1993

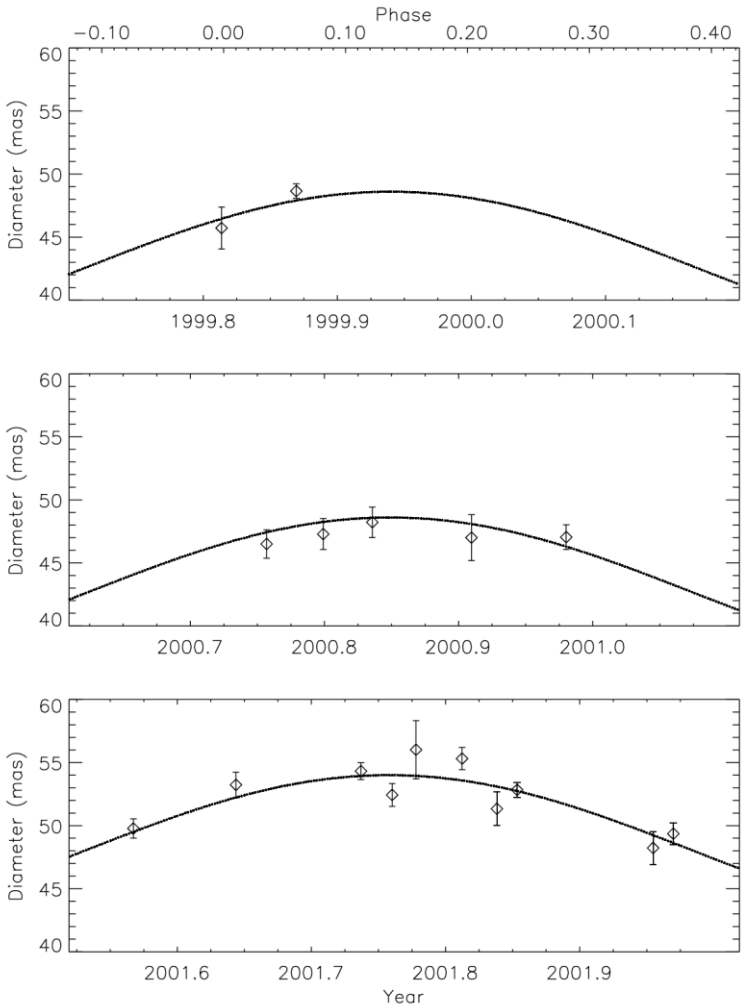

O ceti, Mira
Average diameter 1999-2000, 42.6 mas; 2001, 48 mas
Fitted sinusoid has peak-to-peak amplitude of 12 mas
Max size at visible stellar phase of 0.135

Weiner et al., 2003

Using Phase Closure: Evolution of dust surrounding stars

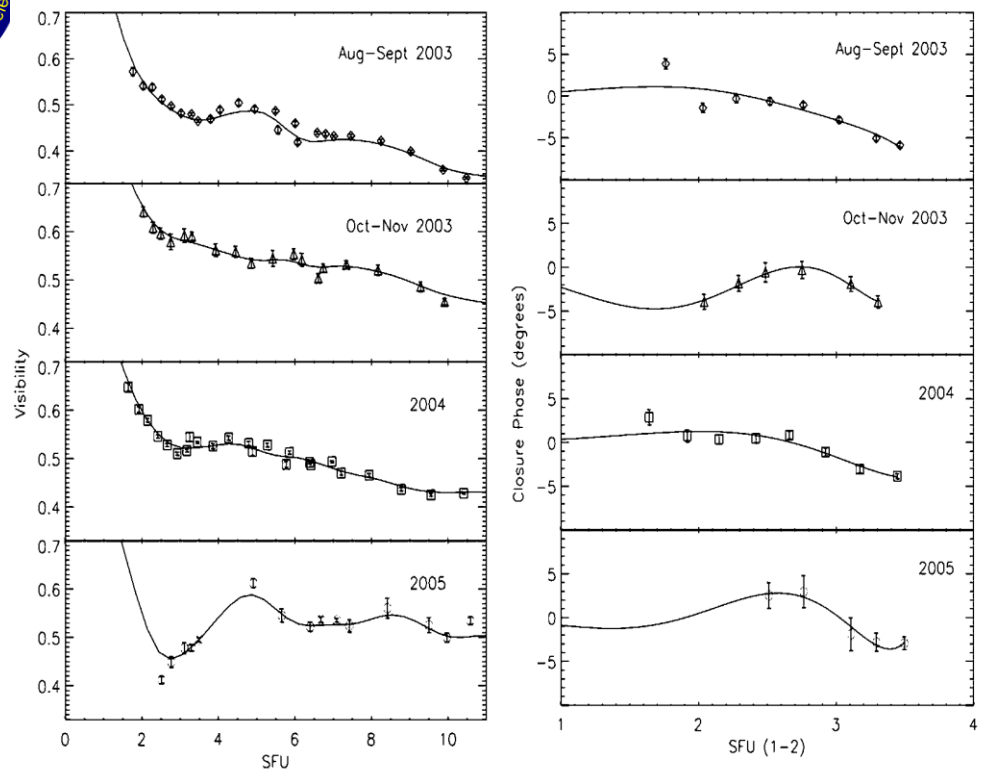

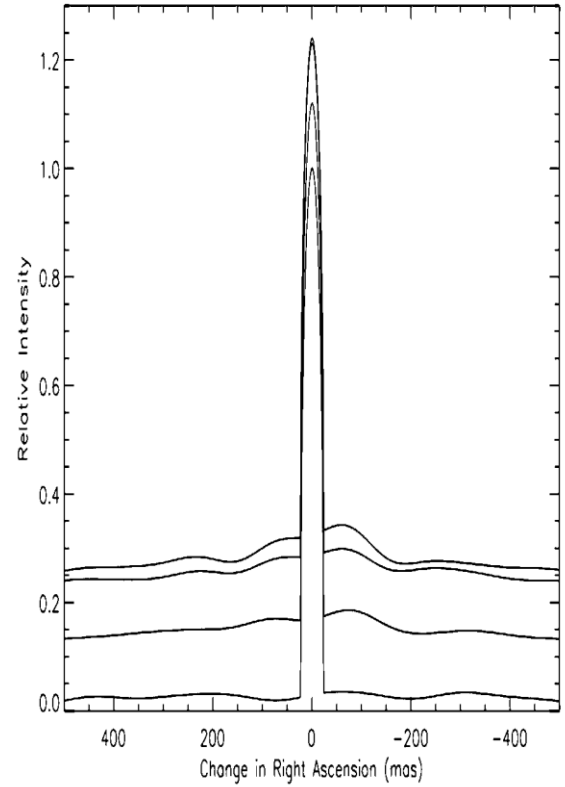

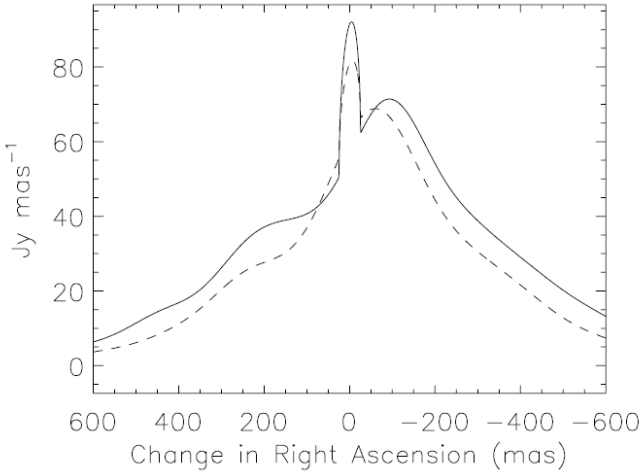

Asymmetry of dust
IRC+10216
2004 (solid)
2006 (dashed)

Chandler et al., ApJ
657, 1042, 2007

In descending order:
Aug-Sep 2003
Oct-Nov 2003
2004
2005

Chandler et al., ApJ,
670,1347, 2007

W Hydrae visibility and intensity dist.

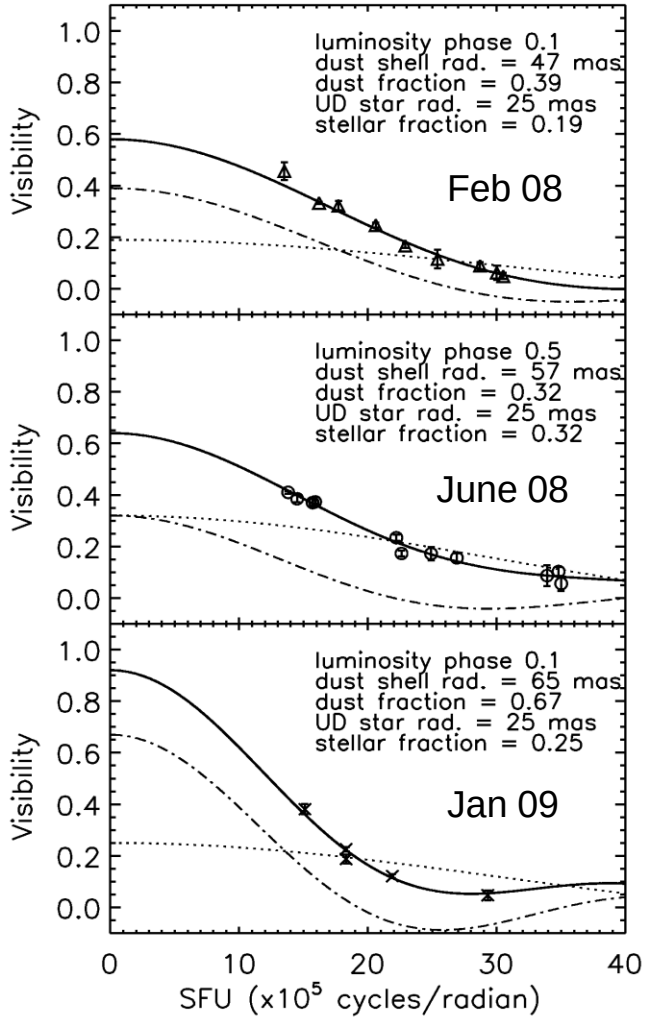

At 104 pc, a 47--65 mas change in radius over a year gives a velocity of 9 km/s

All data including June 1994 & June 1999 fitted with a smooth curve

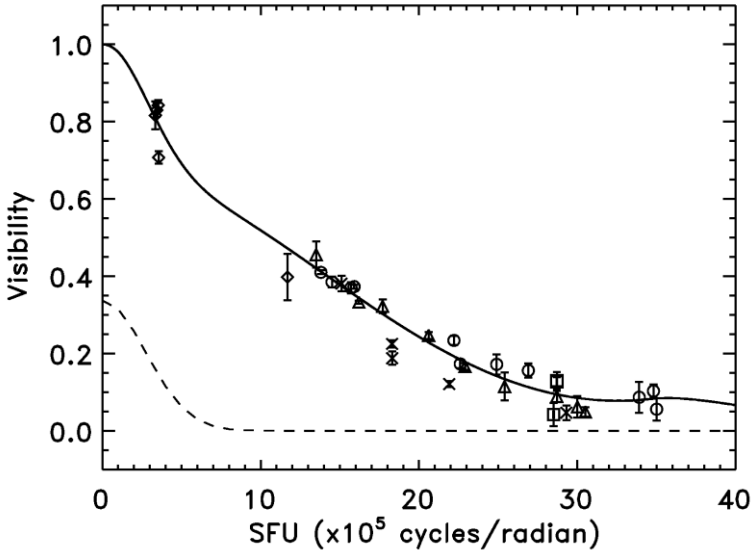

Fourier transform of above curve giving 1-dim. intensity distribution

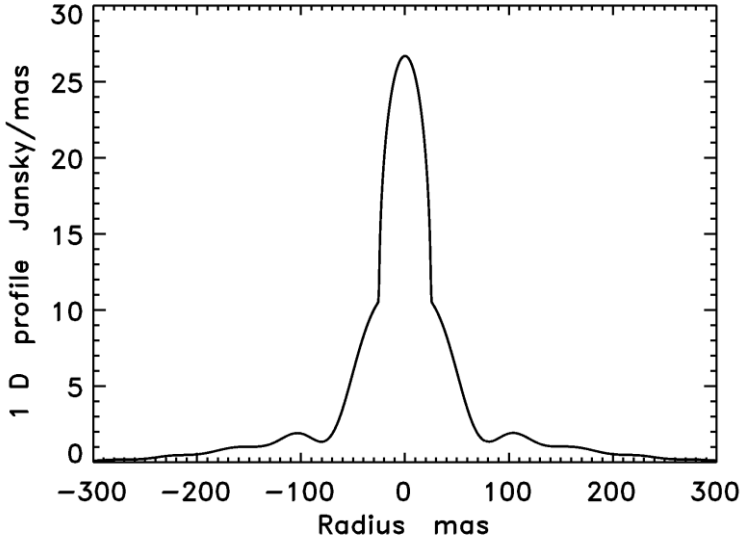

Visibility, phase and model fits of Betelgeuse

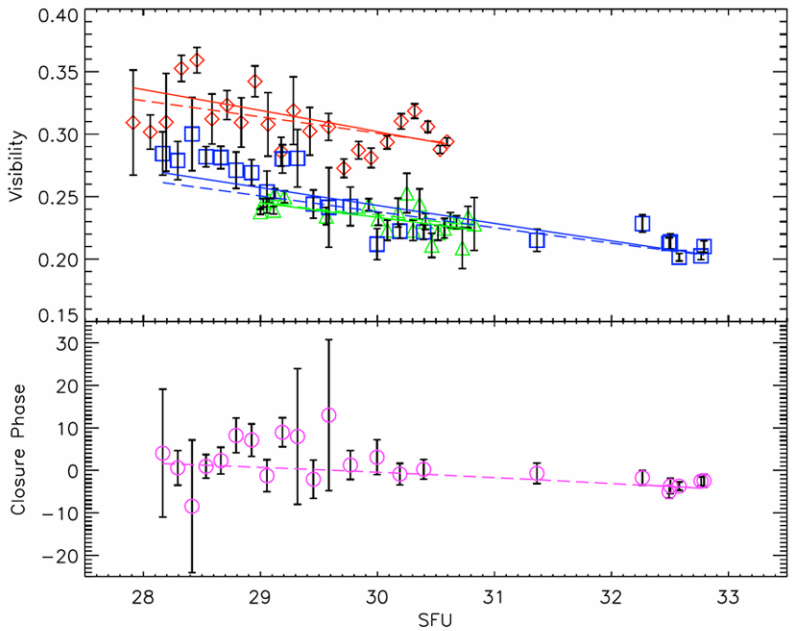

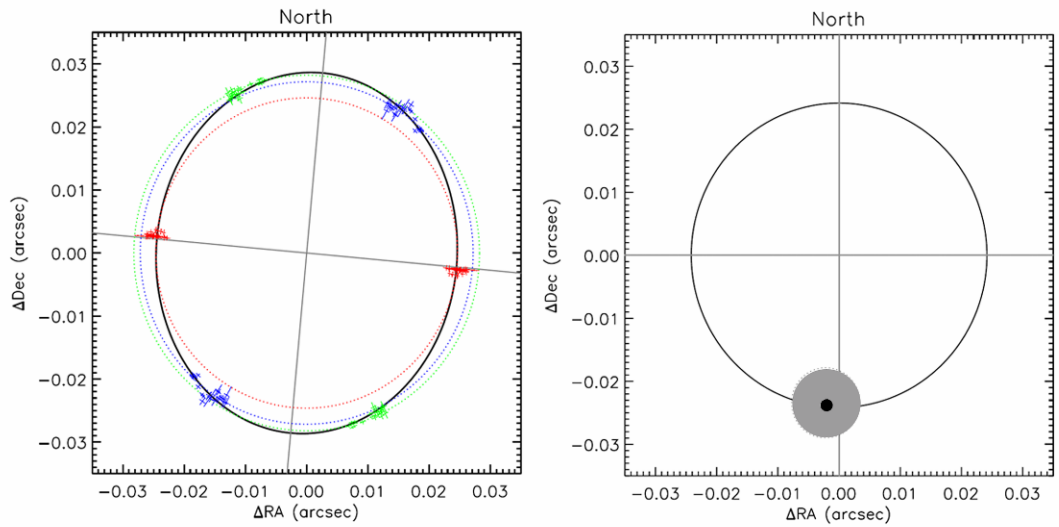

Visibility and closure phase vs. spatial frequency.

SFU is "spatial frequency units" defined as 10^5 cycles/rad

Uniform ellipse model fit to the data. The colors denote different baselines.

Uniform disk+hot spot model fit to the data. The grey circle indicates the size of the spot if it has a surface brightness twice that of the star.

Tatebe et al., ApJ, 670, L21 (2007)

Comparison of mid-IR to radio observations

R Leo ISI
Uniform Disk fits to visibility

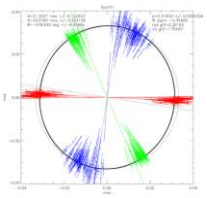

Ellipse 64x62 mas

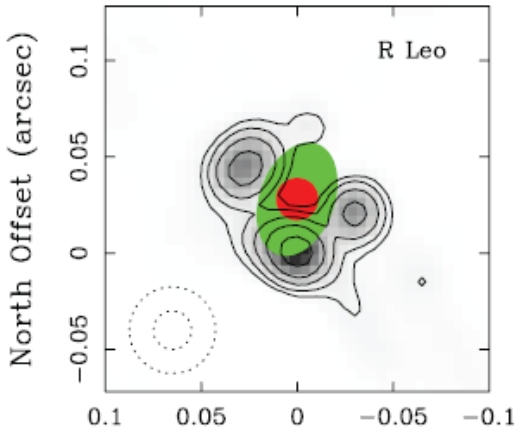

VLA A config
43 GHz, 7 mm
Opacity due to H- free-free
Radio continuum in green
Contours are SiO maser
Ellipse 61x39 mas

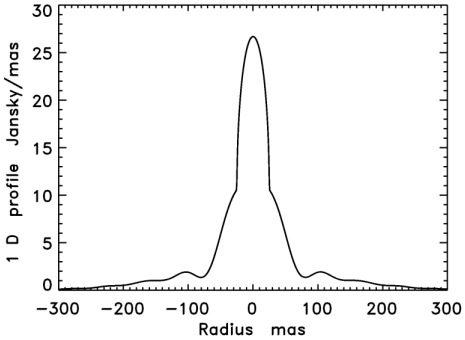

W Hya ISI
1D integrated profile

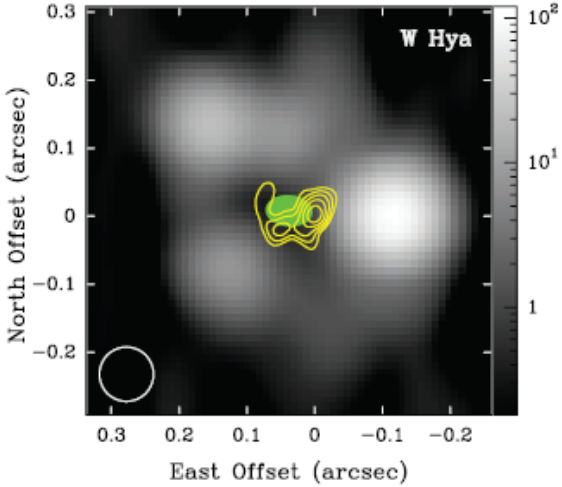

Grey scale is H2O Maser
Emission, 22 GHz

Reid & Menten, 2007, ApJ, 671, 2068

Long term variations of α Her

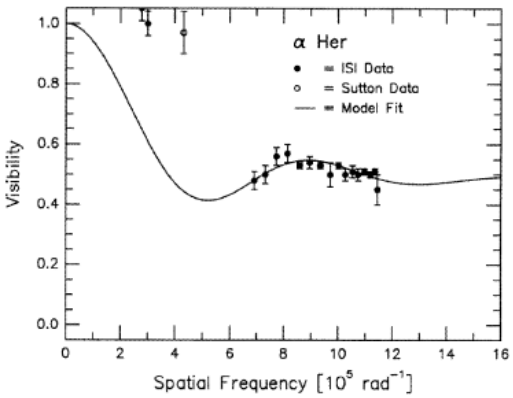

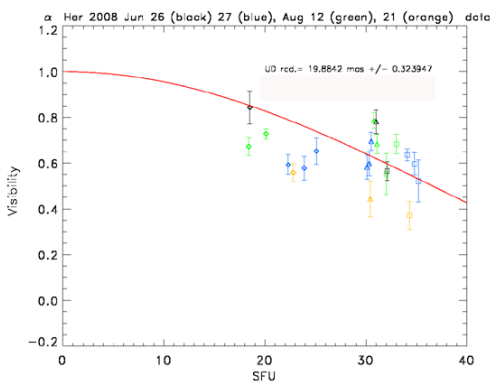

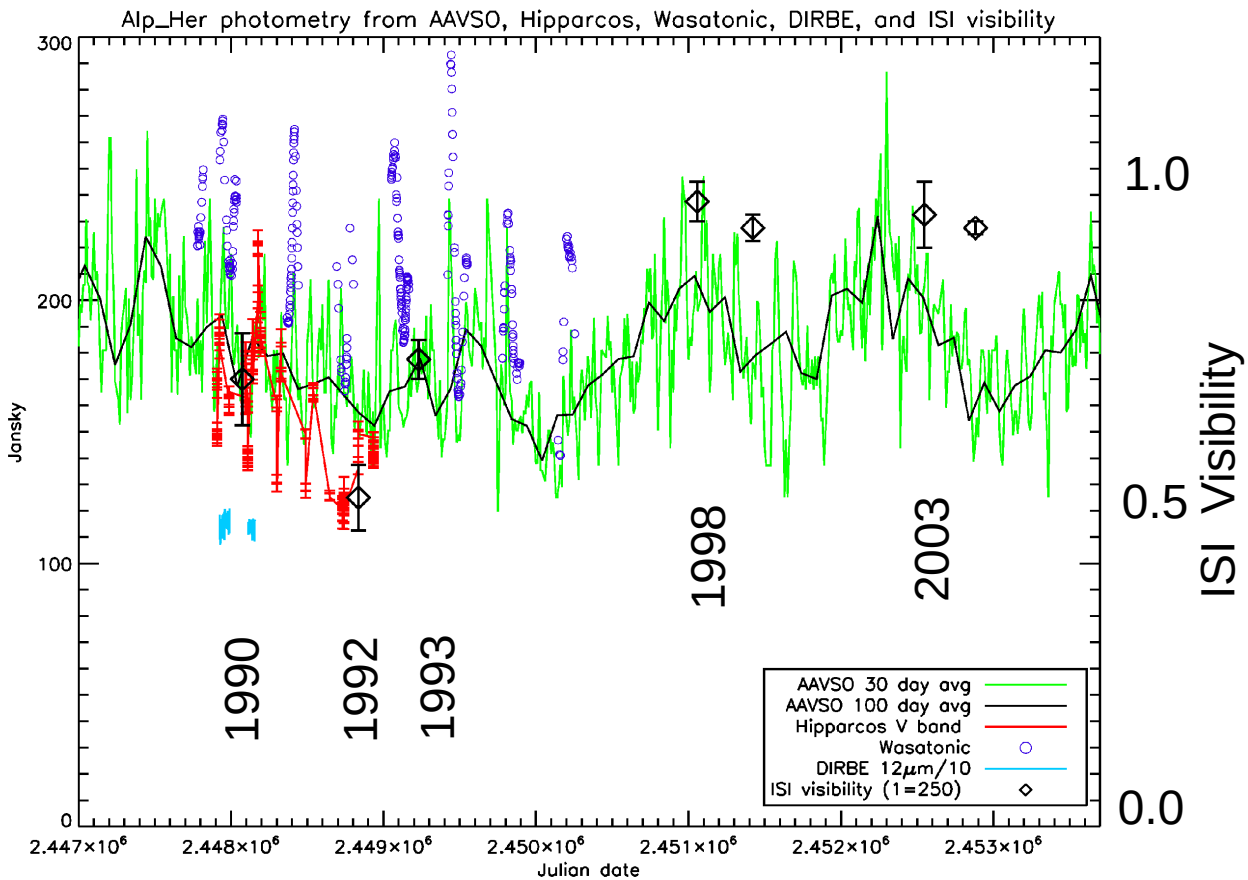

Tatebe et al. "Observation of a Burst of High-Velocity Dust from α Herculis," 2007, ApJ, 658, 103. From 92 to 93, about 75 km/sec

Visibility curves for αOri

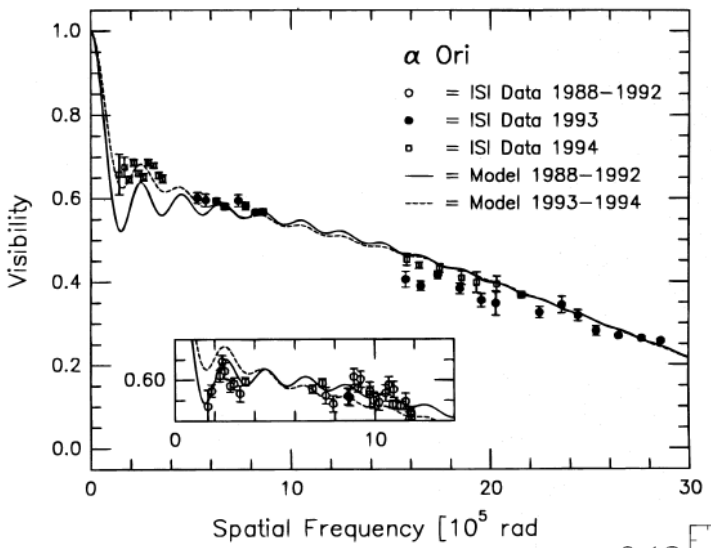

1994 32m baseline
UD diam = 56mas

1999 57m baseline
UD diam = 54 mas

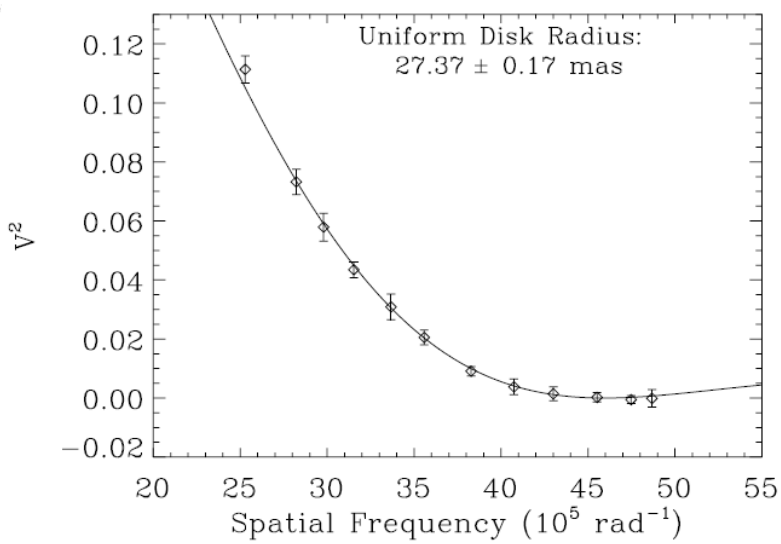

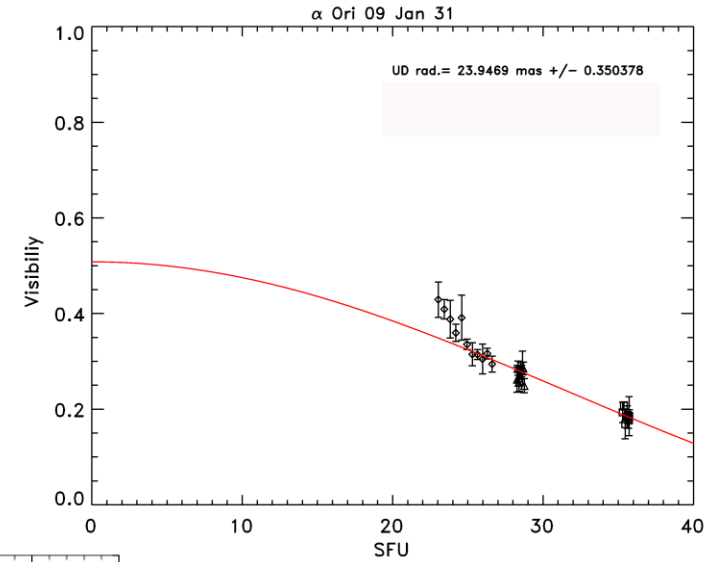

2009 32m baseline
3 telescopes
UD diam = 48 mas

Betelgeuse diameter measured at 11.15 μm 1993-2009

Semi-regular Red Supergiant
M2Iab
Ang. size: ~0."050 diameter
Distance: 197 parsec
(was 131) Harper et al. ApJ, 2008,135,1430
Mass: ~15 - 20 Msolar
Temperature: ~3500 K
Rotation period ~17 years
Surface grav. log(g)~-0.4
~100000 less than solar

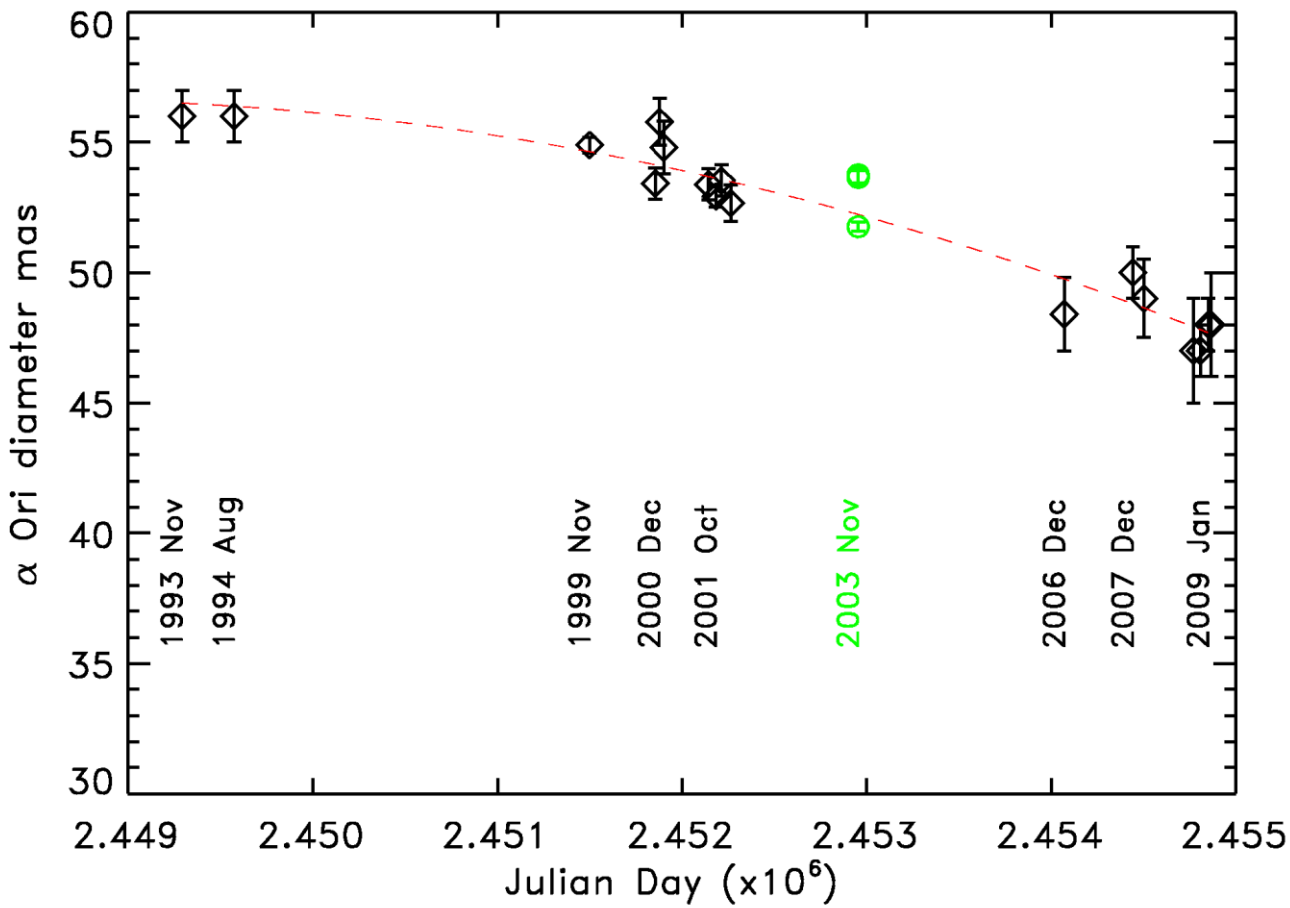

Black pts. Townes, Wishnow, Hale & Walp, 2009, ApJ, 697, L127
Green pts. 10.03, 11.04, 11.15 μm from Perrin et al., 2007, A&A, 474, 599

Comparison to visible photometry

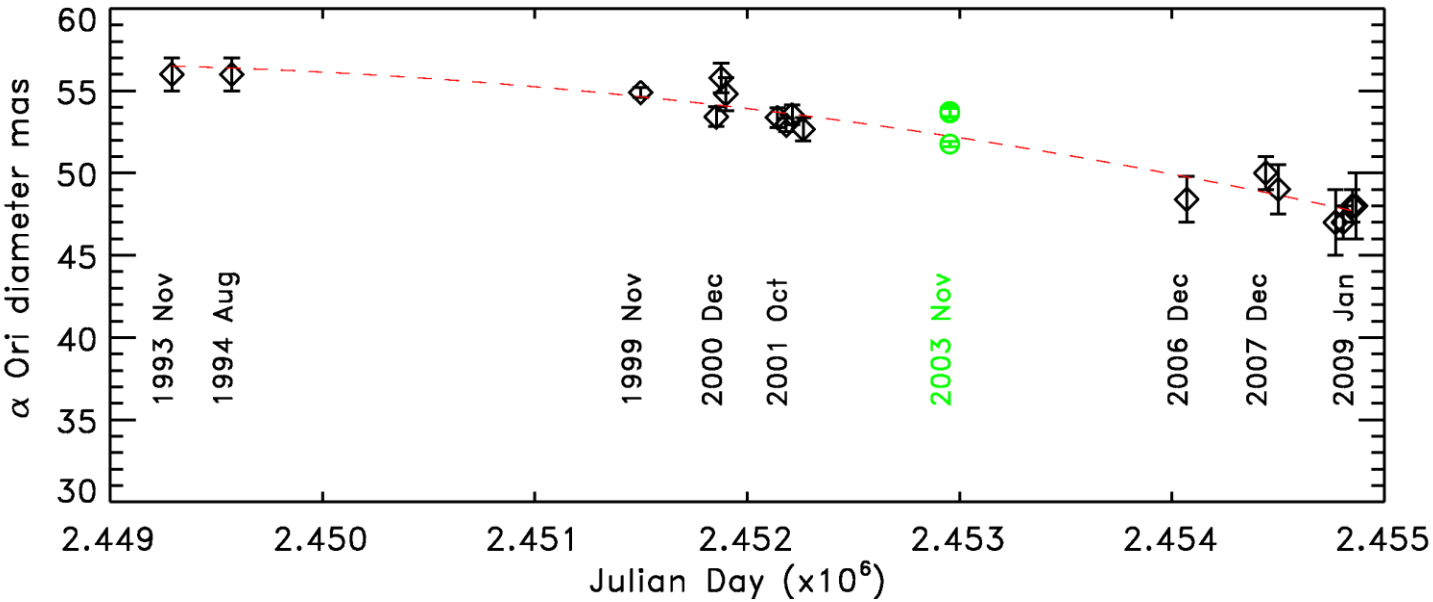

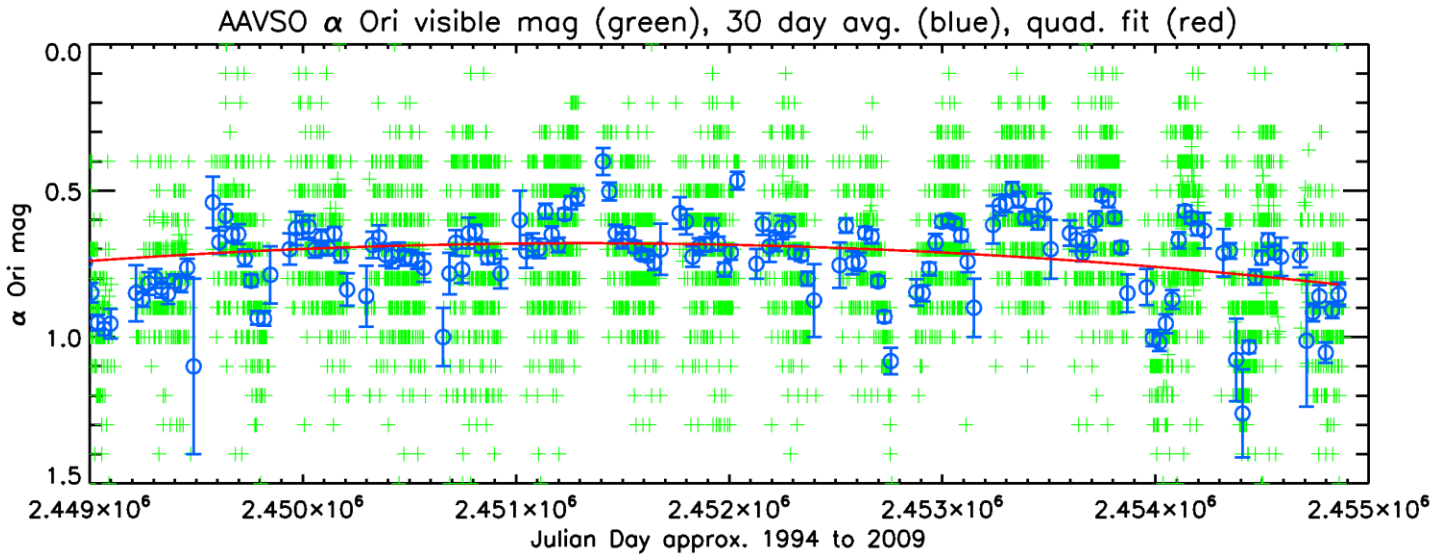

Previous observation of αOri changes

Pease, 1922, 34, 346

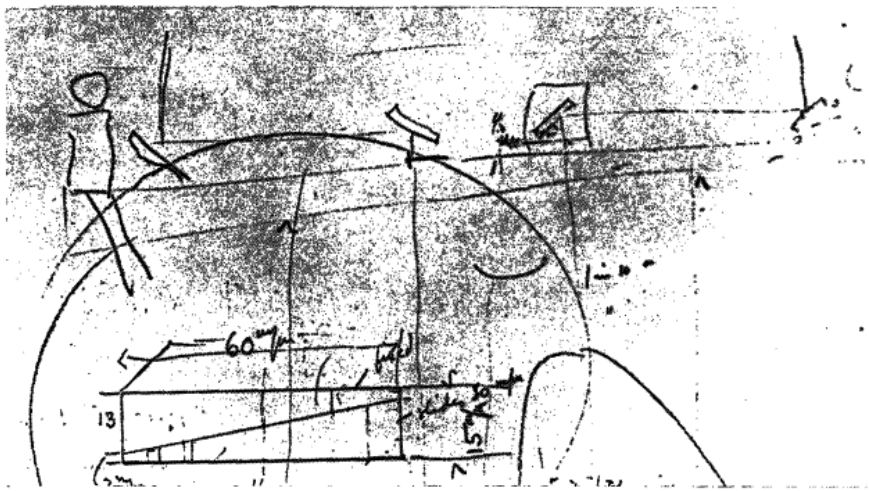

FIG. 3. From F. G. Pease, Notebook 1, sheet 42; approximate date 14 July 1920 (Hale Observatories, copy in Michelson Museum). Crude drawings of the optical wedge used to equalise path length. Note the superimposed sketch illustrating how the night assistant must be perched to move the mirrors on the beam. This situation was necessary because the mirrors, at first, were not continuously adjustable.

Dworkin, J. Hist. Ast., 1975, VI, 1

NOTES ON STAR DIAMETERS:

I. POSSIBLE VARIATIONS IN THE DIAMETER OF α ORIONIS

Further measures have been made on α *Orionis* with the 20-foot interferometer attached to the 100-inch reflector, with the beam extending east and west. On the nights of October 14 and 15, 1922, the visibility curve was found to cross the axis at 14 feet, corresponding to an angular diameter of 0″.034. On the first night the seeing was excellent; on the second night it

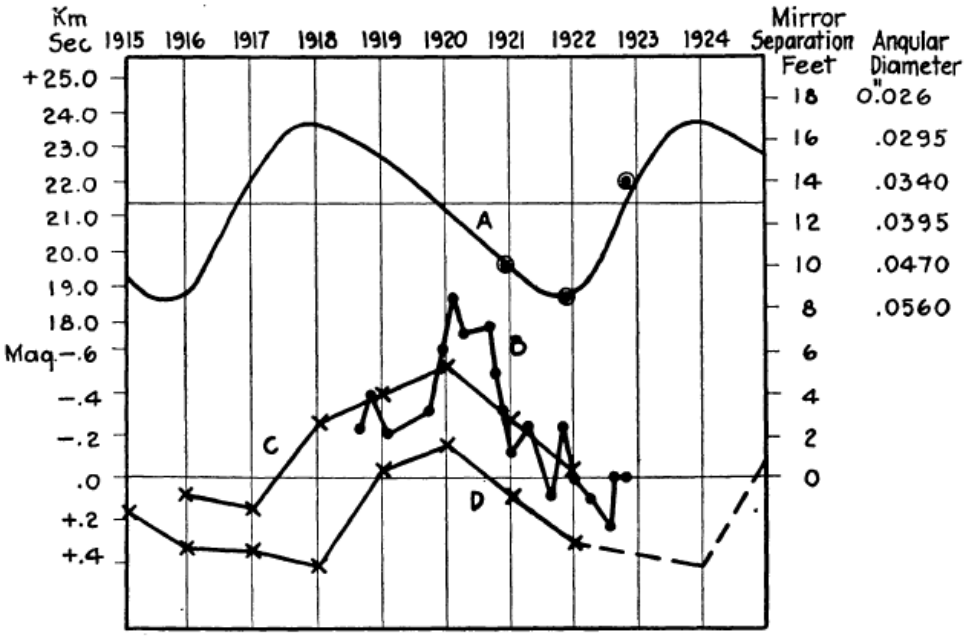

αOri diameter varies w/ wavelength

Narrow band at 11.15 μm avoids effects from spectral lines

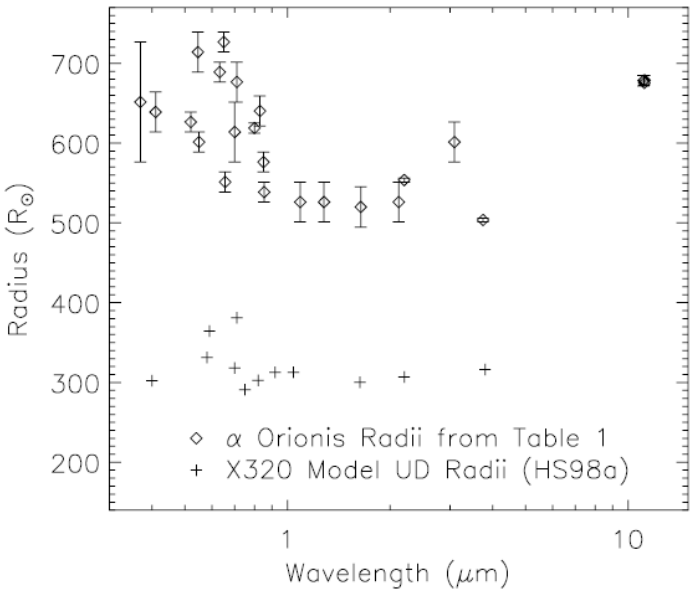

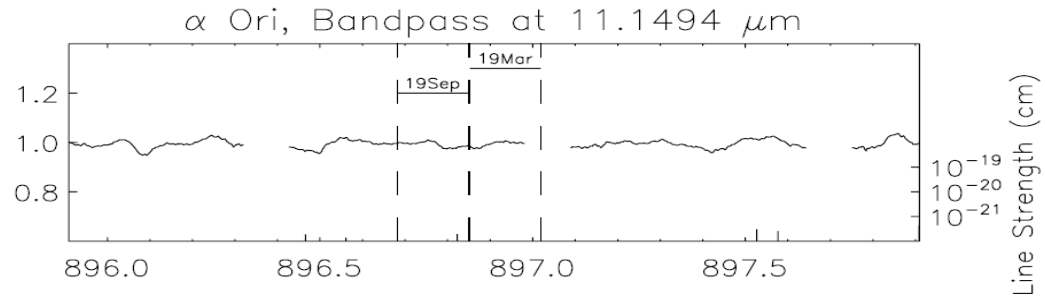

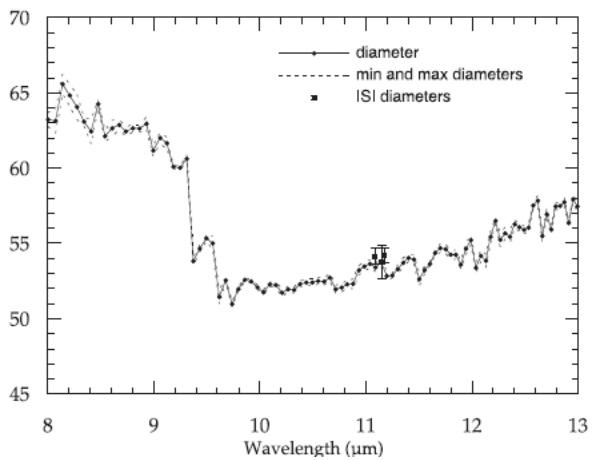

O ceti

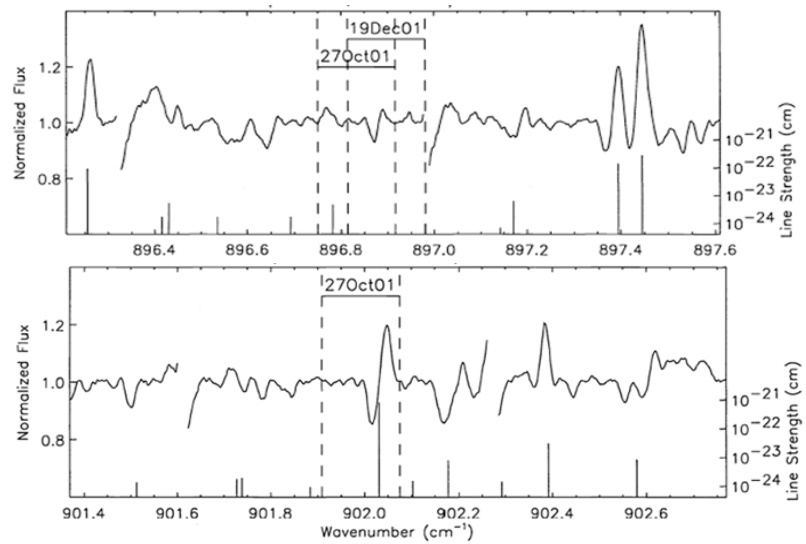

L&R Top: Weiner 2003 ApJ, 589, 976
R Bot: Weiner 2003, SPIE, 4838, 172
L Bot: Perrin 2007, A&A, 474, 599

Comparison of Size and Change in size of Betelgeuse at 11.15 μm to Solar System orbits

FOX NEWS .com Fair & Balanced

Nearby Star May Be Getting Ready to Explode

Nature Blog, "Betelgeuse goes Type II supernova on 21 December 2012 local time. Unlike string theory, this can be validated or falsified"

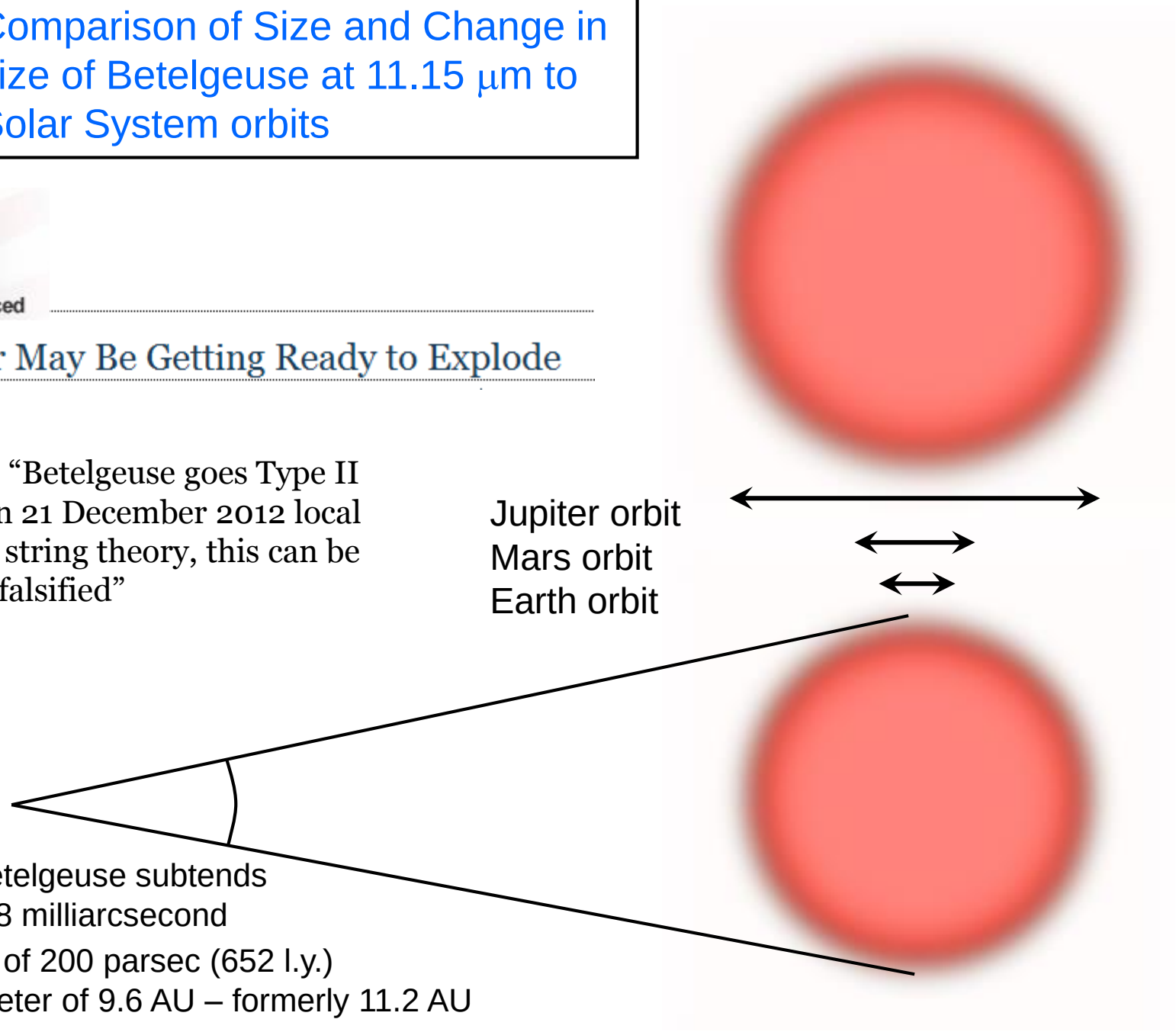

At present Betelgeuse subtends an angle of 48 milliarcsecond

At a distance of 200 parsec (652 l.y.) this is a diameter of 9.6 AU – formerly 11.2 AU

O Ceti, uniform disk fits to visibilities on-off spectral line

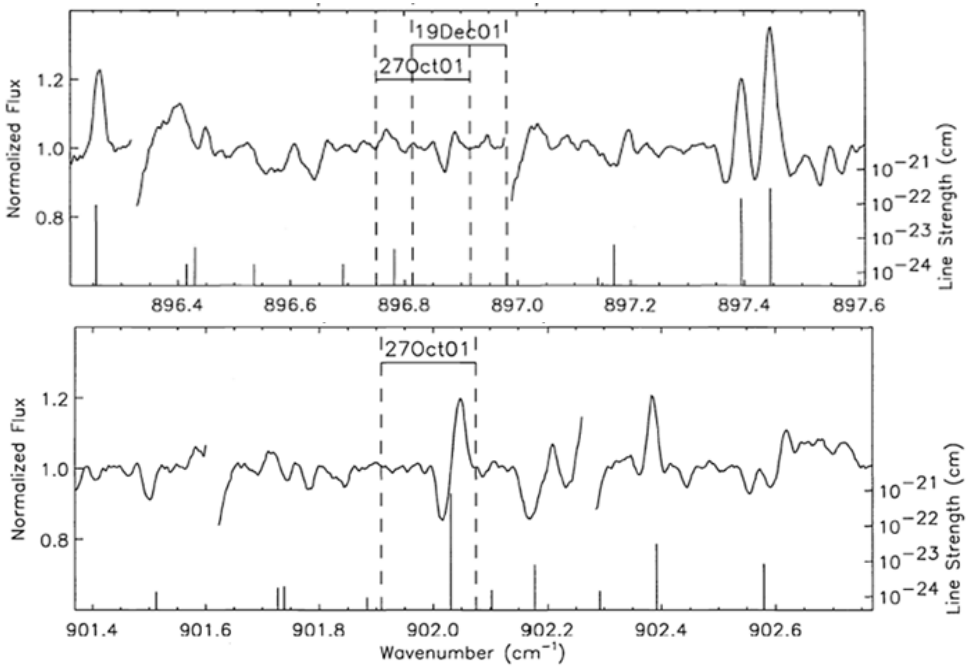

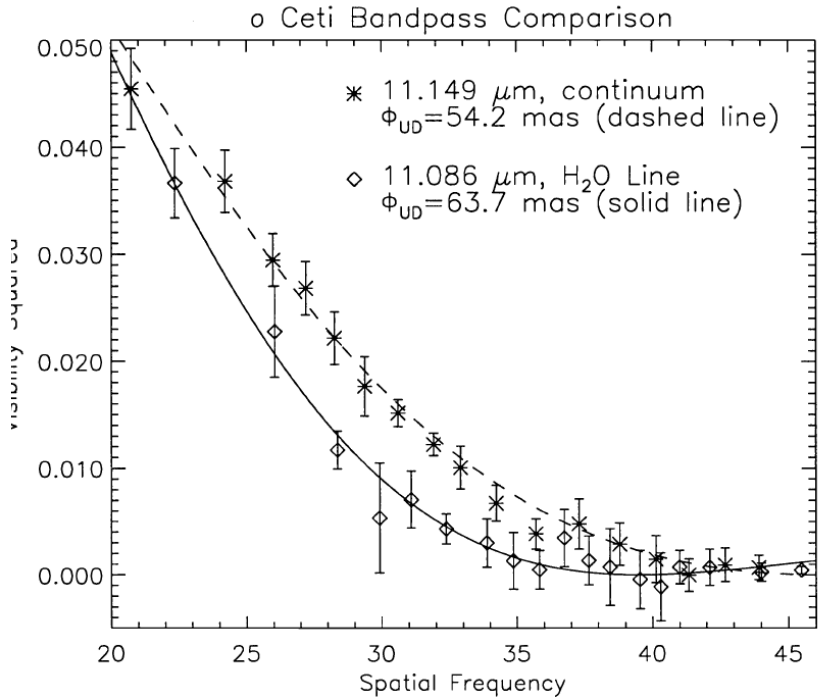

Weiner et al. 2003, SPIE, 4838, 172

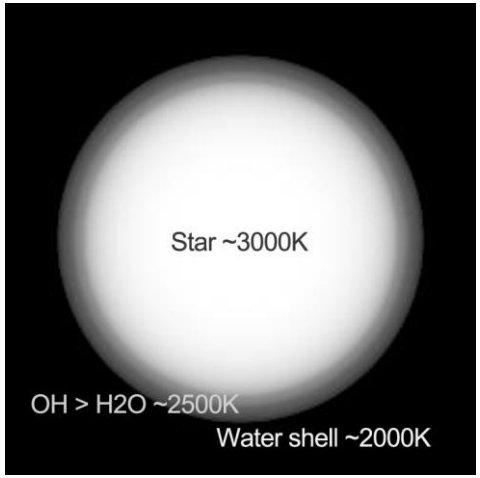

Current system, spectrometer taps A1,A2,A3

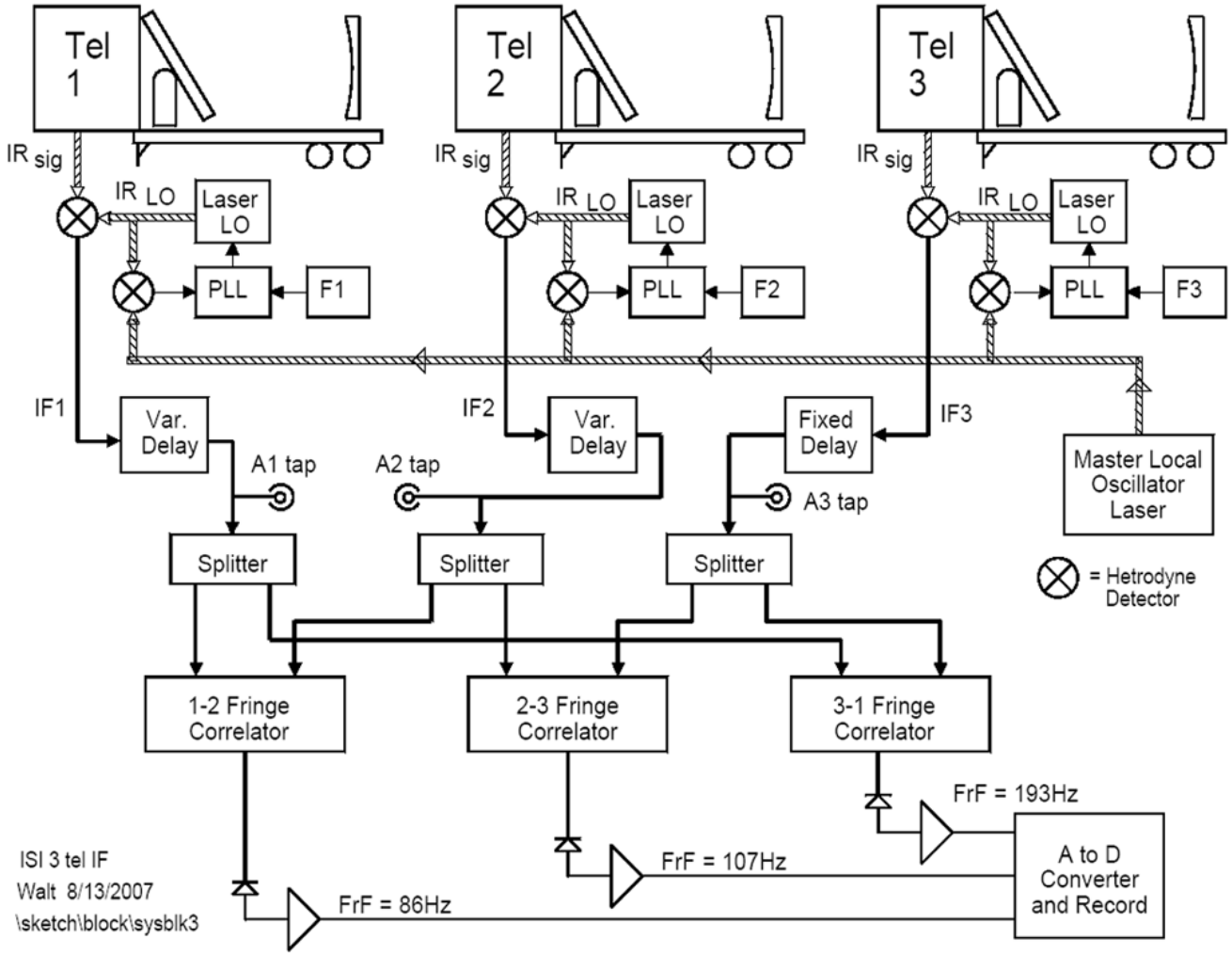

Spectral range covered, lines of interest

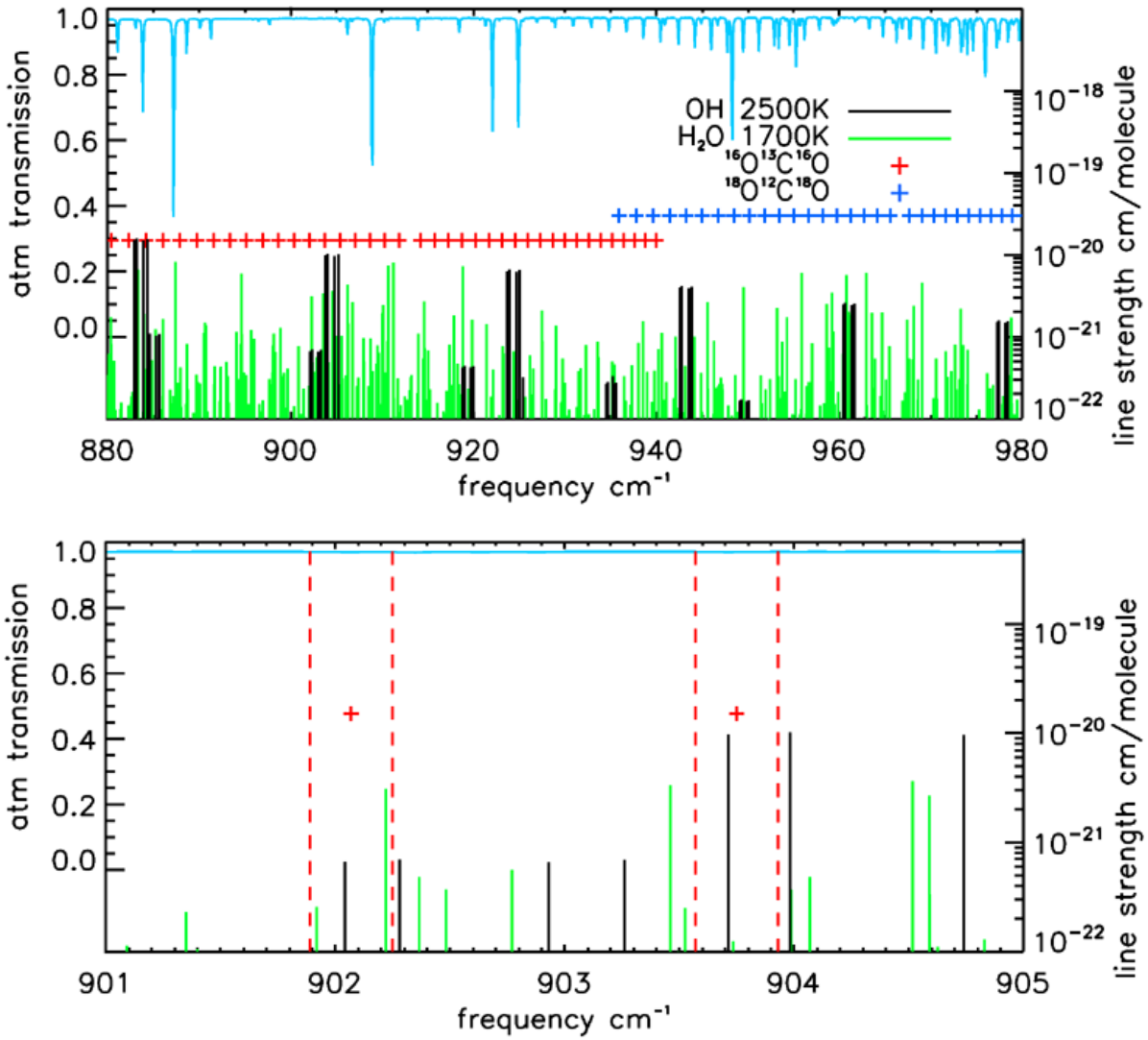

CASPER Center for Astronomical Signal Processing & Electronics Research, Spectrometer/Correlator, Werthimer, Mallard

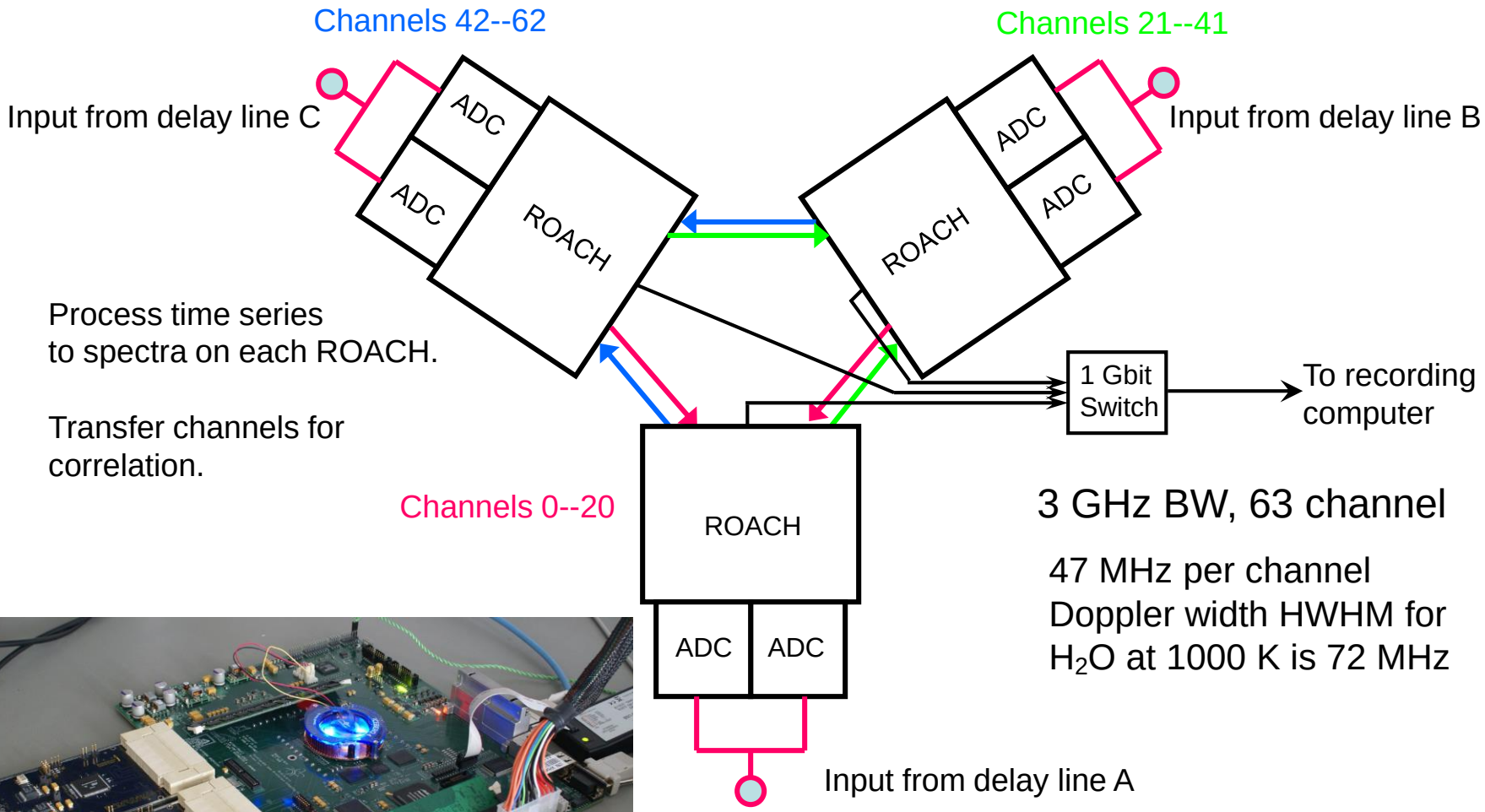

3 GHz BW, 63 channel

47 MHz per channel
Doppler width HWHM for
H_2O at 1000 K is 72 MHz

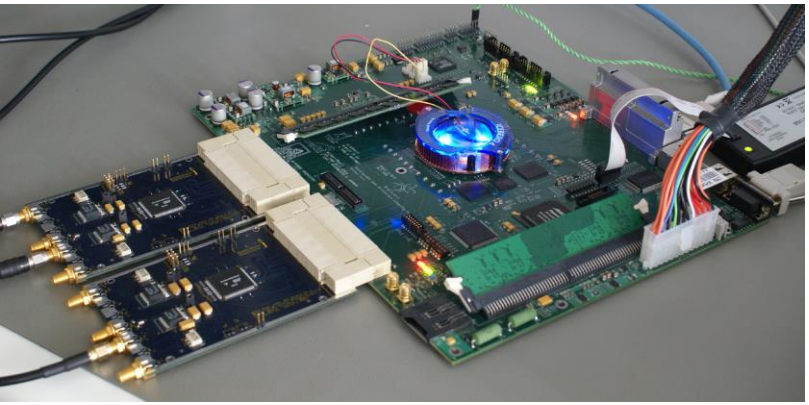

ROACH & ADCs on test bench
Reconfigurable Open Architecture Computational Hardware
Analog to Digital Converter

Testing of 6 GHz ADCs
Casper & SSL: Mallard, Fitelson, Wishnow

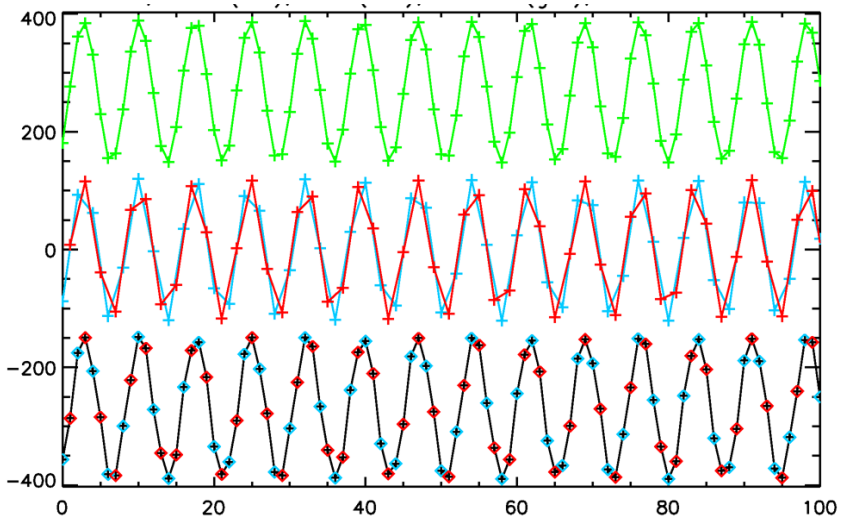

Data from ADC, 6 GHz sampling
Blue even, Red odd samples

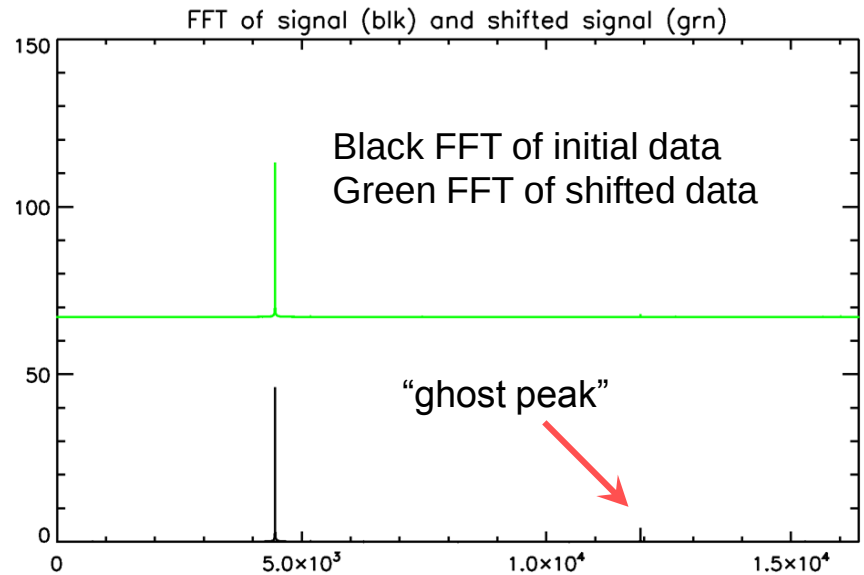

Shift to eliminate ghost, 6 GHz trg= -0.22 samp. int. = 37 ps
Shift to eliminate ghost, 5 GHz trg= -0.18 samp. int. = 36 ps

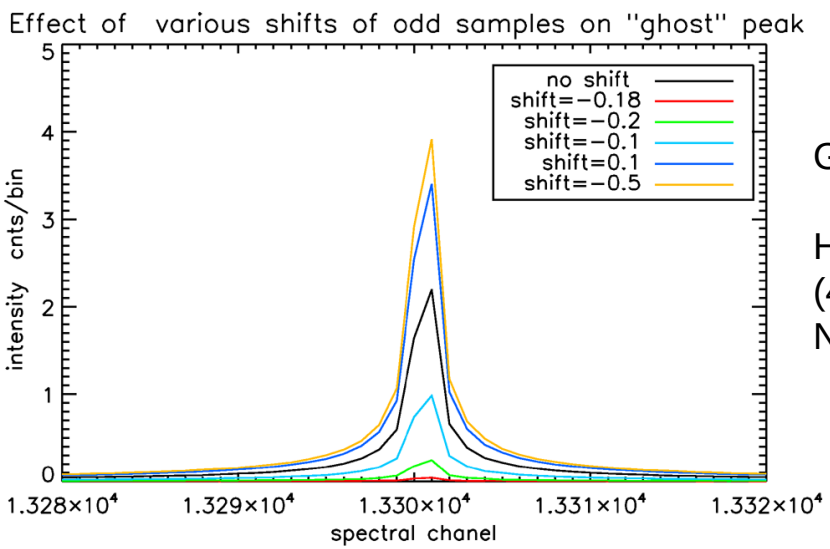

Ghosts at Nyquist – fsignal

Higher order ghosts
(4 fold sampling errors) at
Nyquist/2 +/- fsignal

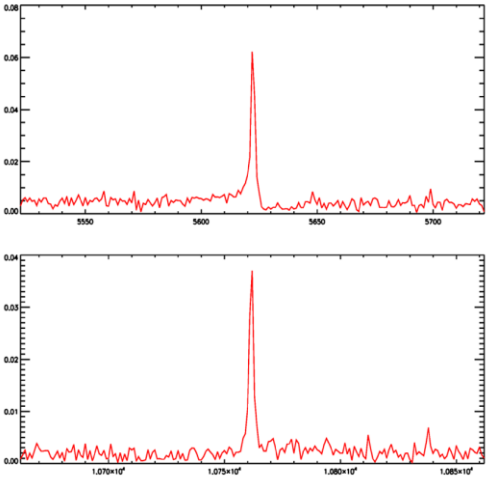

Further examining of ADC interleaved data

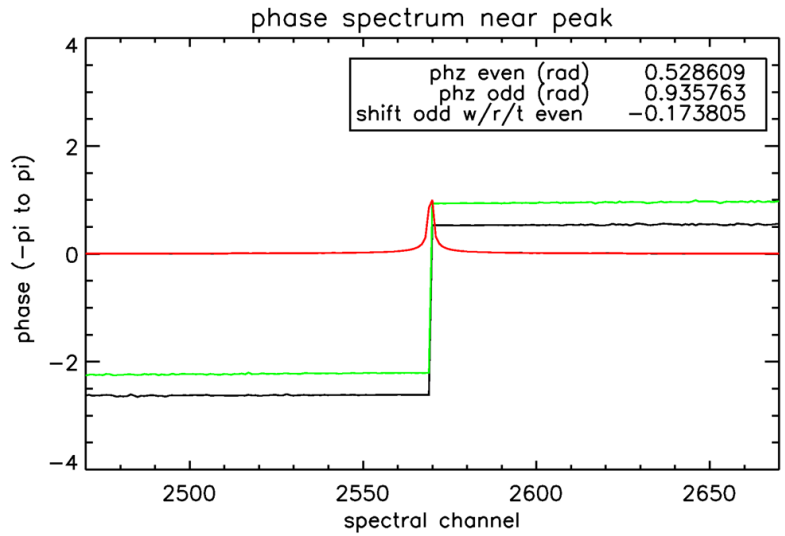

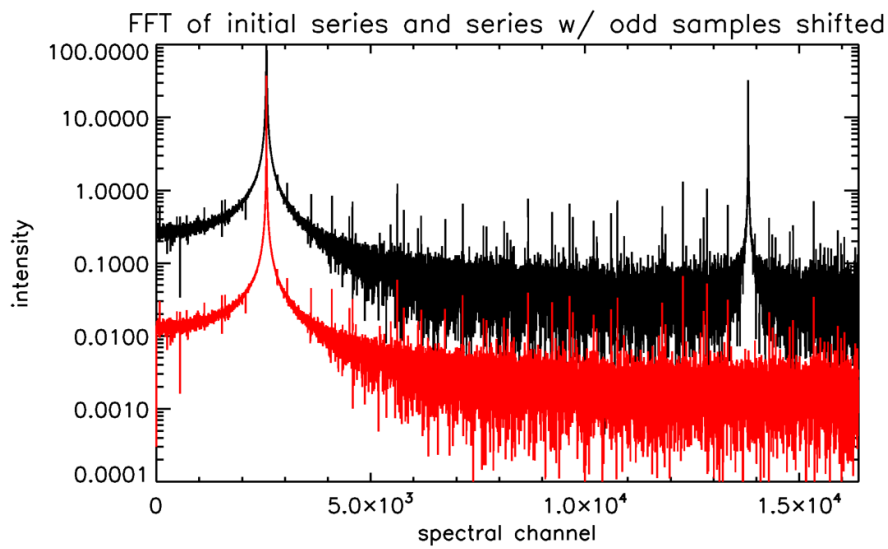

Inject a test signal into the ADC system

Separate the data into even & odd sets

FFT each set (blk, grn) and obtain:
the signal offsets, 0 bins of the spectra
the relative gain, max values of spectra
the phase of the spectra

The phase difference/2pi*signal period gives the phase difference in samples. The phase difference should be unity. The difference from unity is the phase shift of the odd samples.

Black: FFT of input data (shifted upwards)
Red: FFT of data w/ offsets removed, gains balanced, & odd points shifted by -0.173 samp. interval.

Aperture masking interferometry

Peter Tuthill
John Monnier
Bill Danchi
C.H. Townes

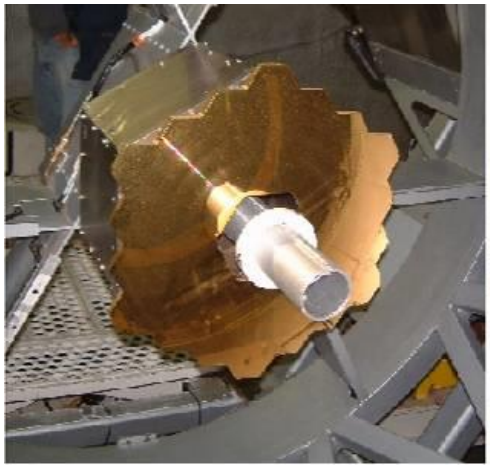

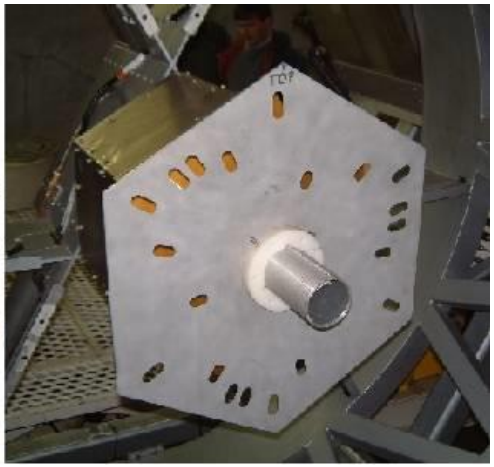

Non-redundant pattern on Keck primary

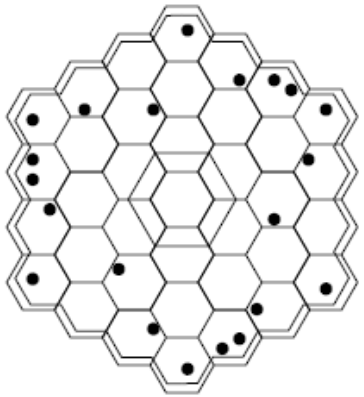

Image recorded at 2.2 μm over short exposure

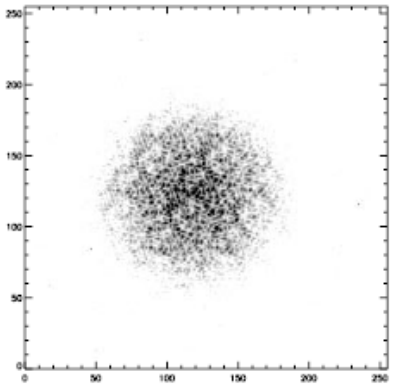

Power spectra from 100 coadded FT of exposures

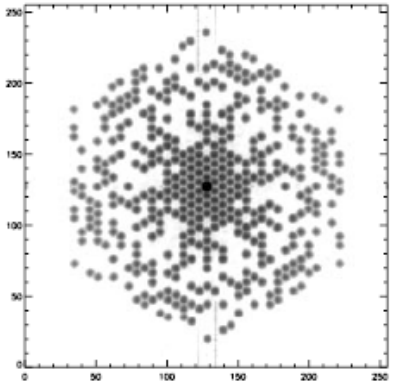

Many samples in UV plane, process much like Radio Astronomy data. Here can also use triplets for Fourier amplitudes and closure phase

Aperture Masking Interferometry

0.1 arcsec
160 parsec

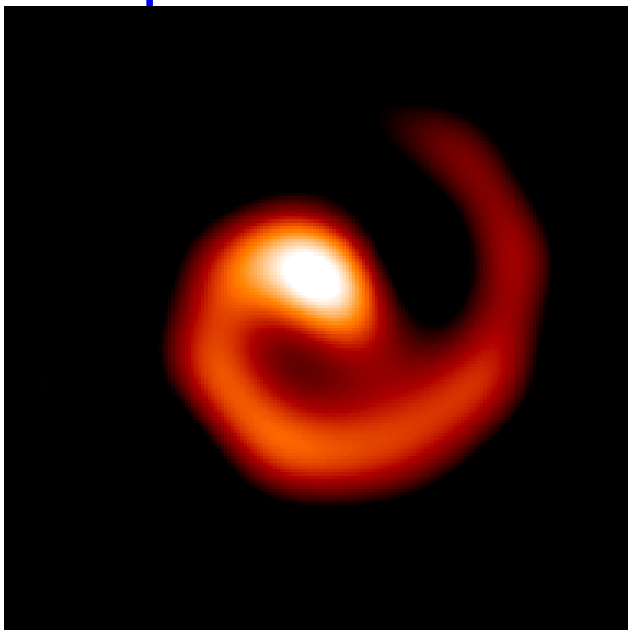

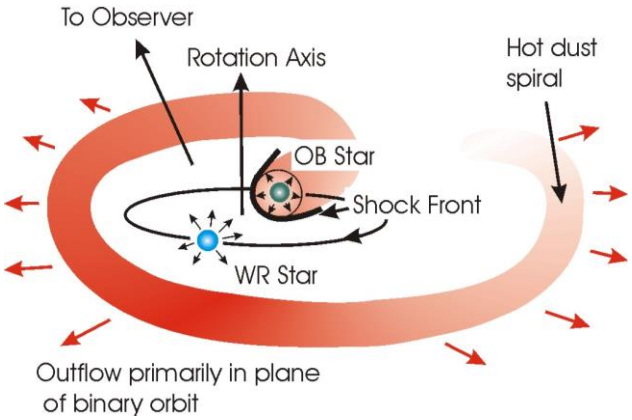

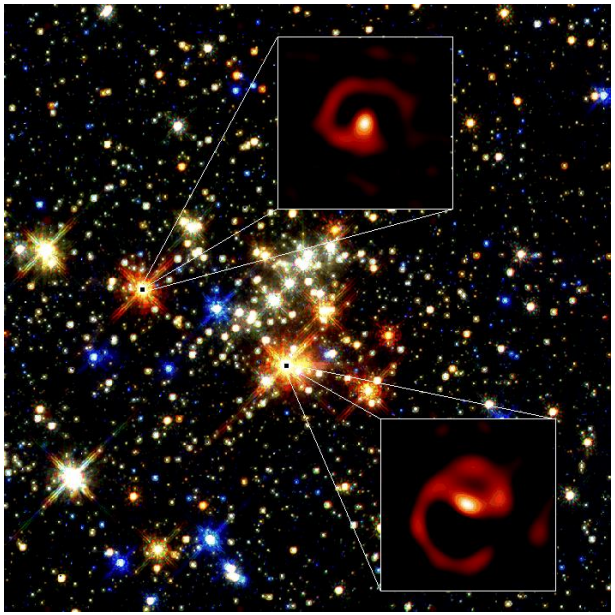

Wolf Rayet 104
Observed on 3 epochs 1998
Nature 398, 487 1999

10 epochs,
Tuthill et al.,
ApJ 2008

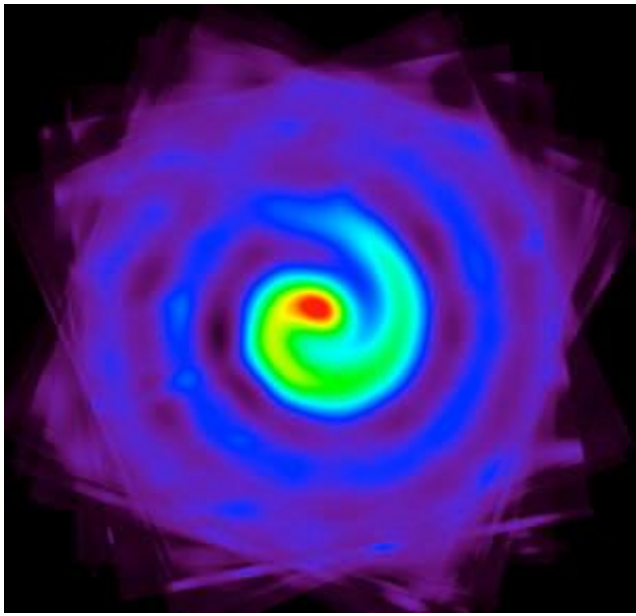

Using adaptive optics,
Quintuplet cluster
Tuthill et al., Science 2006

ISI during a calm winter and an overly exciting summer

Infrared Spatial Interferometer
Space Sciences Lab/UC Berkeley

Charles Townes
Ed Wishnow
Walt Fitelson
Sean Lockwood
Jeff Cobb
Laura Crockett
Hemma Mistry
Dan Werthimer
Billy Mallard